NATIONAL ADVISORY COMMITTEE FOR AERONAUTICS

TECHNICAL MEMORANDUM 1366

HEAT TRANSFER BY FREE CONVECTION FROM HORIZONTAL CYLINDERS IN DIATOMIC GASES

By R. Hermann

Translation

"Wärmeübergang bei freier Strömung am wagrechten Zylinder in zweiatomigen Gasen." VDI Forschungsheft, No. 379, 1936

Washington
November 1954

NATIONAL ADVISORY COMMITTEE FOR AERONAUTICS

TECHNICAL MEMORANDUM 1366

HEAT TRANSFER BY FREE CONVECTION FROM HORIZONTAL CYLINDERS IN DIATOMIC GASES*

By R. Hermann

I. DETERMINATION OF HEAT-TRANSFER LAW FOR HORIZONTAL CYLINDER FROM TESTS WITH PARTICULAR ACCOUNT TAKEN OF THE TEMPERATURE CHARACTERISTIC Te[1]

1. Introductory Remarks

The case of the horizontal cylinder is of particular importance in the study of heat transfer by free convection for the following reasons: in the first place, next to the rectangular plate it represents the simplest two-dimensional case; and second, a very wide range of measurements is possible, from the finest electrically heated glow lamp wires to pipes heated by liquids or gases flowing through them.

To investigate free-convection flow from the point of view of similarity considerations, it is convenient to consider the case of small temperature differences between the heated body and the surroundings; in this case all the properties of the medium, even the density (ref. 1, p. 429), in the entire temperature field may be assumed constant. The case of large temperature differences, for which the variation in properties over the temperature range can no longer be

---

*"Wärmeübergang bei freier Strömung am wagrechten Zylinder in zweiatomigen Gasen." VDI Forschungsheft, No. 379, 1936, pp. 1-24.

[1]Accepted as dissertation by the Technical High School at Aachen with the approval of Prof. Dr.-Ing. C. Wieselsberger and Prof. Dr. W. Muller. The tests were carried out in the division for applied mechanics and thermodynamics of the Physical Institute at the University of Leipzig. The author takes this occasion to thank Prof. Dr. Schiller for the interest which he took in this work and for his valuable advice.

neglected, is treated separately. As first pointed out by W. Nusselt (ref. 2), it follows from the differential equations of free convection, together with the uniquely determining boundary values (ref. 1, p. 428) for the case of small temperature differences, that the nondimensional heat-transfer parameter Nu (Nusselt number[2]) is determined by the lift coefficient Gr (Grashof number) and the characteristic Pr (Prandtl number) for the molecular constitution of the gas[3]:

$$Nu = F(Gr, Pr) \tag{1}$$

where

$$Nu = \alpha d/\lambda, \qquad Gr = d^3 g \beta \Theta/\nu^2 \qquad Pr = \nu/a \tag{2}$$

α is the heat-transfer coefficient $(cal/cm^2)(sec)(^\circ C)$, d is the cylinder diameter (cm), g is acceleration of gravity (cm/sec^2), λ is the heat conductivity $(cal/(cm)(sec)(^\circ C))$, ν is the kinematic viscosity (cm^2/sec), a is the temperature conductivity (cm^2/sec), β is the coefficient of expansion $(^\circ C^{-1})$, and Θ is the temperature difference $(^\circ C)$ between body (t_w) and medium (t_∞).

The case of large temperature difference between the body and the surroundings, for which the gas properties vary over the field, was similarly first considered by W. Nusselt (ref. 2). The following expression is obtained for the heat transfer under the restricting condition that the temperature dependence on ν and a may be represented by exponential laws in the absolute temperature, the exponents of which for gases of the same substance must be equal[4];

$$Nu = F(Gr, Pr, Te) \tag{3}$$

The form here chosen for the temperature characteristic[5]

---

[2]In the notation of the characteristic numbers, the proposals of the Heat Conference at Koln in 1931 are followed. See Forschg. Ing.-Wes., Bd. 2, p. 380, 1931.

[3]See eq. (5).

[4]This is approximately the case, for example, for air, oxygen, and hydrogen; see reference 1, p. 433.

[5]The abbreviation Te is chosen to conform to the other abbreviations for the characteristic numbers and to remind the reader that it refers to a temperature relation.

$$Te = \Theta/T_\infty \tag{4}$$

(T_w, T_∞, ($^\circ$K) = absolute temperatures of the body and the surroundings, respectively) differs inessentially from the nondimensional ratio T_w/T_∞ chosen by Nusselt, namely by the constant -1. Equality of Gr, Pr, and Te in two different cases means complete similarity, that is, similarity of the velocity field, the temperature field, and the field of all the coefficients characteristic of the substance (ref. 1, p. 434), and therefore also equality of the Nu number. The possibility still remains, however, that similarity may exist at the same time that the previously mentioned condition of the power law is not satisfied.

In the present report the characteristics represented in equation (3) will be computed for the heat transfer from heated wires and pipes in air, hydrogen, and oxygen; and from these values the most probable form of the heat-transfer law, obtainable at present, will be determined for the case of the horizontal cylinder in diatomic gases (Pr = 0.74).[5a] The dependence of Nu on the temperature characteristic Te, which follows from the similarity theory and is illustrated by an example (ref. 1, fig. 1) as a third independent variable, will be verified for several tests in the range of Gr from 10^{-4} to 10. For the smallest values of Gr, the effect of Te considerably outweighs that of Gr. In the region of large Gr from 10^4 to 10^7, on the contrary, Te is practically without effect. The large scatter of the test points in the nondimensional representation of the test results of Nusselt (ref. 2) and Davis (ref. 3) (±32 percent in the case of Nusselt) is due to the fact that the parameter Te is not taken into account in accordance with equation (1). The dependence of Nu on Gr, Pr, and Te will be theoretically clarified hereinafter. The effect of Te for small Gr may also be correctly estimated quantitatively.

From the tests conducted by various investigators for different finite Te values, the limiting law of small temperature difference is determined in each case by extrapolation to Te = 0. This is of primary theoretical and practical significance since it is identical with the theoretically simpler case (1) and is thus free from the previously mentioned restrictive assumption with regard to the temperature dependence of the constants defining the properties of the substance.

[5a]For the values of λ and ν required for computing the characteristics, values are assumed for the temperature t_w (in agreement with E. Schmidt). The similarity consideration leaves the choice of the reference temperature free.

2. Radiation

From the measured over-all heat losses directly determined in the tests, the amount due to radiation must be subtracted. For this purpose, a well known equation (ref. 4, eq. 38, p. 232) was employed; the best mean values at present known were substituted as radiation constants for the metal cylinder surfaces, as follows: for platinum, nickel, silver, and tantalum, the values given by H. Schmidt (ref. 5); and for copper and iron, the values given by Gröber (ref. 6, p. 196). Small deviations as compared with the values used by the investigators themselves are without significance in the range of small values of Gr because the radiation component in the case of thin wires amounts to only a few percent of the heat of convection. For the tests of Wamsler and of Koch on thick pipes, however, for which the radiation losses are up to 60 percent, an accurate knowledge of the radiation coefficients is required. These coefficients were obtained by Wamsler (ref. 13) through his own radiation tests. After correction[6] of computations of reference 13, the values obtained herein for the radiation heat are 0.2 to 2 percent larger.

3. Property-Determining Constants of Gases

In order to compute Nu, Gr, and Pr, values of the following properties are required: density ρ, dynamic viscosity μ, heat conductivity λ, and specific heat c for air, hydrogen, and oxygen.

(a) Constants for air. - The density was computed throughout the temperature and pressure range according to the ideal gas law[7].

The true specific heat for constant pressure was obtained from an equation given by Holborn and Jakob[8] for the mean specific heat.

The temperature dependence of the dynamic viscosity was determined by graphical adjustment of the values given by Erk[9]. These values

---

[6]Wamsler (ref. 13) computes incorrectly with the previously mentioned radiation equation without the factor of the area ratio in the denominator.

[7]Landolt-Börnstein: 5th ed., vol. I, p. 43.

[8]Landolt-Börnstein: 5th ed., vol. II, p. 1274.

[9]Landolt-Börnstein: 5th ed., vol. I, pp. 177-181, Eg. I, pp. 143-144, Eg. IIa, pp. 138-141.

differ only slightly (at most, 4 percent) from the graphical mean values given by Erk from 0° to 700° C[10].

The heat conductivity at high temperatures was obtained by a gas kinetic extrapolation, since the test values collected by Jakob[11] lie only between 0° and 212° C. The Nusselt formula (ref. 1, p. 491; ref. 6, p. 192), which deviates from the available test values by at most 2.8 percent, is employed herein.

From the gas kinetic relation[12]

$$Pr = \mu c/\lambda = (n + 2)/(n + 4.5) \qquad (5)$$

where n is the number of degrees of freedom of the molecular motion according to which the Pr number of a gas is independent of the temperature (and moreover is the same for all gases with the same number of atoms); there is obtained for air a small decrease of $Pr = 0.739$ for 0° C to 0.721 at 200° C and 0.679 at 1000° C (value obtained from formula for $n = 5$ is $Pr = 0.737$), which, however, is of no significance because it lies within the uncertainty limits of the μ and λ values. The same holds for the differences in the Pr numbers among air, hydrogen, and oxygen.

(b) Constants for hydrogen and oxygen. - For the kinematic viscosity and heat conductivity the values given by Davis (ref. 3) are employed, which also for air are in good agreement (deviation, at most 2.7 percent) with the chosen values. A knowledge of the specific heat is unnecessary if the Pr value for 0° C is satisfactory; the values are 0.717 for hydrogen and 0.731 for oxygen[13].

(c) Gas constants for high pressures. - From the tests of Petavel, which extend up to 160 atmospheres, only those up to 40 atmospheres were computed in order that reliable gas constants would be available. In this pressure range and up to 1000° C, the computation was conducted

---

[10]Wien-Harms: Handb. d. Exp. Phys., IV, 4, p. 531.

[11]Landolt-Börnstein: 5th ed., vol. II, p. 1304.

[12]A. Busemann in Wien-Harms: Handb. d. Exp. Phys., IV, 1, p. 359. This relation may be obtained from an equation given by Eucken (Physik Z., vol. 14 (1913), p. 324.

[13]A. Busemann in Wien-Harms: Handb. d. Exp. Phys., IV, 1, p. 362.

with the normal values since the dependence on the pressure of λ and μ and the deviations of ρ from the ideal gas law are either not known at all or are only partly known, and the known deviations amount to only a few percent[14].

4. Individual Investigations[15]

(a) General. - The nondimensional representation of the results is effected according to equation (3) by logarithmic graphs with Nu as a function of Gr and with Te as the only parameter, since Pr (according to sec. 3a) may be considered as constant. Even if the slight variation of Pr there indicated is considered as real, there would, according to a test result of Davis (ref. 3) on the effect of the Pr number, be obtained only displacements of the curves of the order of magnitude of 1/100 of those which can actually be observed.

In table I are summarized the test objects and test conditions of the individual investigators and the range of Te used. In order to judge to what extent the condition of infinite extension of the fluid was satisfied, the ratio of the height H of the surrounding space to the cylinder diameter d is shown. In figures 1 to 7, approximately equal Te values are indicated by the same symbols. The decrease in Nu with increasing Te is particularly evident in the individual point groups (because of the same wire), whereas the values for different wires naturally show larger scattering as compared with one another. The curves Te = constant were obtained by a graphical adjustment process and, similarly, the extrapolation points and curves for Te = 0 and the dependence of Nu on Te (relative decrease in Nu for ΔTe = 1). The indicated minimum and maximum values hold for the individual wires (point groups); the indicated mean values, for the individual investigators.

(b) Results of Ayrton and Kilgour (ref. 1), figure 1. - The authors of reference 1 give in the form of diagrams for each wire the total heat-transfer coefficient as a function of the wire temperature; two wires (0.0206 and 0.0282 cm diam.) because of the very large scattering and a third wire (0.0102 cm diam.) because of its strong deviation in position and inclination were excluded from the evaluation of the tests. The

[14]Landolt-Börnstein: 5th ed., Eg. I, p. 64 ff, Eg. IIa, p. 144.

[15]Acknowledgement is made to Dr. K. Winkler, Leipzig, for his assistance with the computations.

points computed from the low temperatures of 40° to 80° C were similarly not used on account of the large scattering.

(c) Results of Langmuir (ref. 8), figure 2. - Langmuir gives in a table the adjusted values of the total energy losses as a function of the absolute wire temperature increasing in stages of 200° C. Only the tests up to 1300° K were computed herein in order to have reliable values available for ν and λ. The convergence of the curves $Te = 1.33$ and $Te = 3.33$ shows that the dependence of Nu on Te decreases with increasing Gr, the decrease independently determined for the individual wires being:

log Gr	0.1-4	0.8-4	0.6-3	0.5-2	0.4-1
Decrease, percent	7.2	7.5	5.4	3.2	2.2

This experimental confirmation of the results following from theoretical considerations (sec. 6b) acquires significance in that the tests of Langmuir are characterized by a large change of the Te number and smallest scattering. The extrapolation from $Te = 1$ to $Te = 0$, on account of the absence of test points for this value, was effected with the mean value of 13.2 percent taken from reference 7.

Langmuir (ref. 9) also discusses his own tests at various air pressures (10 to 760 mm Hg) and variable room temperature (t_∞ = -190° C to 600° C) which on account of the strong change in the expansion coefficient ($\beta = 1/T_\infty$) would be of great interest and the only tests of their kind. Unfortunately, these tests have not as yet been published, and the test data are not available in a form in which they may be evaluated[16].

(d) Results of Bijlevelt (ref. 10), figure 3. - Since the tests of Bijlevelt were primarily for the purpose of investigating forced convection, the experimental setup was designed for the sensitivity requirements of this flow. This explains the greater scatter of the test points of reference 10 as compared with those of other investigators. For each individual wire (with the exception of the Ta and Ni wire), a grouping is nevertheless observed with respect to Te in the usual sense.

(e) Results of Kennelly, Wright, and Bijlevelt (ref. 11), figure 4. - The investigation of reference 11 is noteworthy in that through the pressure (ρ,ν) changes, even for constant wire diameter and constant surrounding temperature, a change is effected in the Gr number so that

[16]For these data the author is indebted to a personal communication from Dr. I. Langmuir.

curves of Te = constant are here obtained from tests on a single wire. The nondimensional representation of these tests (fig. 4) has been given previously (ref. 1). The authors give for each wire a diagram with the heating current as a function of the pressure for three or four different temperature differences, as parameter of which the values for five different pressures were computed in terms of the characteristics and were connected by the curves Te = constant. The extrapolation to Te = 0 shows extremely good agreement for both wires. The values of the wire of medium diameter (d = 0.02616 cm) were not plotted because of the irregularities obtained.

(f) Results of Petavel (ref. 12), figure 5. - From the over-all heat-transfer coefficients given for constant pressure as a function of the temperature difference, values were computed for 200°, 400°, 600°, 800°, and 1000° C temperature differences up to pressures of 40 atmospheres. For the sake of clarity, however, only the curves for the extreme Te values are plotted in figure 5. Since the heat conductivity and density of hydrogen differ from the values of air by the factors 6 and 14, respectively, these tests would have been particularly suitable for checking the similarity law. Unfortunately, however, these tests are evidently unreliable because of the far too small jacket pipe (H/d = 18.6 as the smallest value of all investigators). The similarity law for the three gases is confirmed only for Te = 0.69 and $Gr > 10^2$. In the case of air and oxygen, there is a splitting with respect to the dependence on Te, but in the reverse sense from that observed for all wires of the other investigators. In the case of hydrogen, a dependence on Te in the correct sense is observable only at the smallest values of Gr. Finally, the Nu values also for small Gr lie too high as compared with the values of all other investigators and the rise in the Nu with increasing Gr has too great a lag. For these reasons, the results of Petavel for determining the heat-transfer law were not used.

(g) Results of Wamsler (ref. 13), figure 6. - Wamsler's curve, which was obtained on the basis of correctly computed radiation loss (sec. 2), shows a dependence on Te such that the mean values for Te = 0.60 lie about 5 percent higher than those for Te = 0.20. This small splitting of the effect of Te which occurs in the opposite sense to that in the case of small Gr, however, in all probability does not contradict the facts but may be explained by the consideration that the radiation coefficients in the entire temperature range from 50° to 270° C were assumed constant, whereas in general for metals there has been established an increase of the radiation coefficient with the temperature. If in the previously mentioned temperature range a rise in the radiation coefficients of about 5 percent is assumed, as follows for cast iron from Wamsler's determination of the radiation coefficient and for wrought iron from the determination of Nusselt (ref. 14), the observed splitting of the effect of Te is neutralized and the curve shown, valid for all Te values, is obtained. The test values of the

copper pipe and of a wrought iron pipe (of 5.9-cm diam.) were not employed in figure 6 because of the obvious irregularities indicated by the scattering.

(h) Results of Koch (ref. 15), figure 7. - The nondimensional characteristics were redetermined herein with the values λ and ν for wall temperature, since the characteristics given by Koch were computed for a mean temperature of the substances. The test results show an unusually small scattering which is to be ascribed a careful accounting for various factors (e.g., determination of the temperature of the air in the room and at the walls, and also the end effect of the pipes). For the two intermediate pipes, after graphical adjustment, a decrease of Nu for Te = 0.07 to 0.52 by about 2.5 percent is observed, whereas in the case of the smallest pipe no ordering is observed and in the case of the largest pipe there is a partial decrease and a partial scattering. In agreement with the results of Wamsler, the dependence on Te is thus practically zero also for large Gr (10^4 to 10^7).

5. Summary of Test Results

The results of the different investigators as regards their agreement may be compared in two groups. In the region of small Gr (10^{-4} to 10), the tests of Ayrton and Kilgour, Langmuir, Bijlevelt, and Kennelly and coworkers are in agreement. From these investigations are determined, on the one hand, the curves Te = 0 for the limiting law of small temperature difference (fig. 8) and, on the other hand, the curves Te = 0.65 corresponding to an intermediate test range (fig. 9). For Te = 0 the maximum scatter of the results of the four investigators is 10.5 percent, the minimum 5 percent, the corresponding values for Te = 0.65 being 22 and 8.5 percent, respectively. The middle curves of figures 8 and 9 obtained for Te = 0 and Te = 0.65 give for this change in Te an average change in Nu of 14.7 percent (fig. 10). A relative decrease in the Nu number by 22 percent with increase of Te from 0 to 1 is thus obtained as the experimental mean value of the effect of Te for small Gr.

In the region of large Gr (10^4 to 10^7), the test values of Wamsler and Koch from energy measurements and the values obtained from the temperature field measurements of Jodlbauer (ref. 16) by integrating over the cylinder perimeter are shown in figure 10. As follows from the discussion of the results of Wamsler and Koch, the values of Koch must be considered as more reliable. There is nevertheless an uncertainty in the values due to the uncertainty in the radiation components which lie between 40 and 60 percent. On the other hand, the temperature field measurements of Jodlbauer are free from this source of error. Since, moreover, the results of reference 16 are in good

agreement (mean deviation, 4 percent) with the theoretical solution given in Part II they were assigned a greater weight in the evaluation. Jodlbauer himself, however, considers his energy measurements, which are about 10 percent higher and lie near the values of Koch, to be correct and his field measurements in error because of the introduction of the thermocouple. The test points of Wamsler are, on the average, 18 percent higher than the theoretical values, and those of Koch, 11 percent higher. The interpolation curve is not everywhere satisfactory as regards its slope and curvature and could be determined only with a partial deviation from the test values.

The differences still existing, after extensive adjustment, among the individual investigators and the difficulty of interpolation show that the heat-transfer curve is still not conclusively determined with the desirable accuracy of several percent, but that, on the contrary, further tests are required. The given interpolation curve nevertheless represents the most probable curve of the heat-transfer law, obtainable at the present time, for diatomic gases with account taken of the dependence on Te in the range of Gr from 10^{-4} to 10^{7}. The numerical values of this curve are given in table II.

6. Qualitative Theoretical Interpretation of Heat-Transfer Law

(a) Streamlines. - It is necessary to explain theoretically the dependence of the Nu number on Gr and Te, determined experimentally in sections 4 and 5 (fig. 10), and also the dependence on Pr as obtained by A. H. Davis (ref. 3) for liquids. A solution of the differential equations under the assumption of a thin (as compared with the cylinder diam.) heated laminar layer is given in Part II for diatomic gases (Pr = 0.74) and small temperature differences (i.e., approximately constant properties, Te ≈ 0) and is valid for mean values of Gr of about 10^{4} to 3×10^{8}. On the basis of these theoretical results and with the aid of suitable assumptions, the dependence of Nu on small and large Gr and also on Pr and Te will be discussed theoretically without any necessary implications of finality in the conclusions.

The streamline plot (fig. 11) obtained from the solution and the isotherms of figure 12 show that cold air streams from the bottom and sides of the cylinder with increasing velocity in laminar flow upwards along its surface, is deflected away from the surface in the region of the upper stagnation point, and forms a rising current of warm air. With increasing Gr of the cylinder, the thickness of the streaming layer relative to the cylinder diameter decreases. Since the velocities increase at a higher rate, however, the Reynolds number Re of the boundary layer increases so that the boundary layer finally becomes turbulent. According to the schlieren photographs of figure 23, this occurs in the neighborhood of the upper stagnation point at $Gr = 3.5\times10^{8}$.

With further increasing Gr, the point of turbulence transition travels upstream (fig. 26) and reaches the equatorial region at $Gr = 3 \times 10^9$. With decreasing Gr of the cylinder, the Re of the boundary layer likewise decreases, and at the same time the thickness of the layer in relation to the cylinder diameter increases so that the given solution of the differential equations finally (below $Gr = 10^4$) becomes invalid. At very small Gr (very small Re), the isothermal picture of the free flow in the neighborhood of the body becomes increasingly similar to the concentric isothermal picture of the pure heat conduction[17] so that almost static heat-conduction relations may here be supposed. An estimate of the Te effect made under this assumption at small Gr likewise gives good agreement with the measurements (see following section b). The following fundamental difference is nevertheless to be observed. For initially given cylinder temperature and heat transfer, the solution of the heat-conduction equation has as the potential function at infinity a singular point (negatively infinite temperature). That is, even at a very large distance from the cylinder the room temperature continues to decrease, whereas actually in the case of free flow the room temperature at large distance from the body very soon becomes constant.

(b) Heat transfer. - Dependence on Gr. For the dependence of Nu on Gr, the solution of the differential equations under the familiar assumptions of the Prandtl boundary-layer theory gives

$$Nu \sim Gr^{1/4} \tag{6}$$

as is also approximately shown by the tests of Wamsler and Koch (fig. 10). At very large Gr with at least partial turbulent flow, the heat transfer must rise more strongly on account of the increased mixing. With increasing turbulent mixing the dependence of the heat-transfer coefficient on the position must also decrease. The assumption that α is independent of the position (or on the cylinder diam.), as is obtained from the tests of Griffiths and Davis (ref. 17) for a vertical plate, gives on the basis of dimensional considerations

$$Nu \sim Gr^{1/3} \tag{7}$$

Above $Gr = 3.5 \times 10^8$, the proportionality of the Nu number to the fourth root of Gr corresponding to the upstream travel of the point of transition to turbulence must gradually become a proportionality to the cube root. Experiments of W. King (ref. 18) on vertical cylinders,

[17] See photographs by R. B. Kennard; Bur. Stand. J. Res., vol. 8 (1932), p. 787. Report on this by M. Jakob: Forschg. Ing.-Wes., vol. 4 (1933), p. 45.

plates, and blocks at Gr up to 10^{12} confirm the cube-root law as already pointed out by M. Jakob and W. Linke (ref. 19). For very small Gr, for which the amount of heat transferred by convection is always below that transferred by conduction, the Nu number in accordance with its definition must gradually become constant, as may be seen from the discussion of data below $Gr = 10^{-3}$ (fig. 10).

Dependence on Pr. The dependence of Nu on Pr for Gr = constant and Te = constant may be understood by assuming a change in λ with all the remaining magnitudes kept constant. The increase in Pr, through a decrease in λ, gives in the region of predominant heat conduction (very small Gr) a proportional decrease in the quantity of heat transferred, that is, Nu = constant. In the region of large Gr, a decrease in λ (on account of the smaller conduction component as compared with the convection component) gives a relatively smaller decrease in α, that is, an increase in Nu. In agreement, investigations by Davis (refs. 3 and 20) on liquids of very different Pr (Pr = 0.74 to 7940) for small Gr give the limiting value of Nu which is independent of Gr and also of Pr. For medium and large values of Gr, an increase of Nu with Pr was obtained.

Dependence on Te. The dependence of Nu on Te for Gr = constant and Pr = constant for diatomic gases is determined by the temperature dependence on λ, ν, a, and also by the temperature chosen in computing the characteristics Gr and Nu (Pr is independent of the temperature) for the fluid properties λ and ν ($\beta = 1/T_\infty$ is constant in the entire field, ref. 1); the wall temperature t_w or T_w was chosen herein.

An increase of $Te = (T_w/T_\infty)-1$ is considered to be due to a decrease in T_∞ with T_w constant so that the values of λ and ν employed for the computation of Nu and Gr remain unchanged. The associated increase of β and Θ is compensated by a decrease in the gravity field g so that $g\beta\Theta$, that is, the lift acceleration and Gr remain constant. Hence colder outer layers with smaller λ and ν but larger ρ now take part in the heat transfer. In the region of very small Gr with predominating heat conduction λ, the magnitude α, and hence Nu, must therefore decrease with increasing Te. This is also shown by the data discussed previously between $Gr = 10^{-4}$ and 10 (see fig. 10). For the region of very large Gr with smaller viscosity and heat-conduction effect as compared with the turbulent momentum and heat mixing, it also follows[18] from the momentum equation,

[18]Under the reasonable assumption that with the change of Te the profiles of the velocity and temperature to a first approximation undergo affine variations. The 'standard velocity W' may thus be taken for example as the maximum value of the tangential velocity at the equatorial region of the cylinder.

because of the constancy of the lift acceleration, that the standard velocity W is constant. The participation of colder layers with increased value of ρ in the heat transfer here means an increase in the heat-transfer coefficient α, which is proportional to $c\rho W$, and therefore in Nu.

The decrease of Nu with increasing Te for very small Gr contrasts, therefore, with an increase for very large Gr. The effect of Te for small Gr values must therefore, in agreement with the test results of Langmuir, first decrease with increasing Gr values and finally, somewhere in the range of medium Gr, must practically vanish, as is evidently the case according to the experiments between $Gr = 10^4$ and 10^7 (fig. 10).

For the range of very small Gr, the order of magnitude of the dependence of Nu on Te under the approximating assumption of purely static heat conduction may be estimated when a mean conductivity is used,

$$\lambda_m = \frac{1}{T_w - T_\infty} \int_{T_\infty}^{T_w} \lambda(T)\,dT \tag{8}$$

the following expression is obtained for the Nu numbers corresponding to two different Te values Te_1 and Te_2 for equal wall temperature $T_{w_1} = T_{w_2}$:

$$\frac{Nu(Te_1)}{Nu(Te_2)} = \frac{\lambda_m(Te_1)}{\lambda_m(Te_2)} \tag{9}$$

The value $Te_1 = 0$ is chosen, that is, vanishing temperature difference or $T_{w_1} = T_\infty$; and $Te_2 = 1$, that is, $T_{w_2}/T_{\infty_2} = 2$. For the temperature dependence of λ, the previously (ref. 1) given exponential form is used[19]

$$\lambda/\lambda_0 = (T/T_0)^n \tag{10}$$

with $n = 0.738$[20]

[19] λ_0 is the value of λ for the arbitrarily chosen temperature T_0.

[20] Determined from the previously given exponent for a of 1.738 neglecting the temperature dependence on c.

From

$$\lambda_m(Te_2) = \frac{1}{T_{w_2} - T_{\infty_2}} \int_{T_{\infty_2}}^{T_{w_2}} \lambda \, dT$$

with $T_0 = T_{w_1} = T_{w_2}$ in equation (10) and by integration:

$$\lambda_m(Te_2) = \frac{\lambda(T_{w_1})}{n + 1} \cdot \frac{T_{w_2}}{T_{\infty_2}} \cdot \frac{T_{\infty_2}}{T_{w_2} - T_{\infty_2}} \left\{ 1 - \left(\frac{T_{\infty_2}}{T_{w_2}} \right)^{n + 1} \right\}$$

Since $\lambda_m(Te_1) = \lambda(T_{w_1})$, the following expression results after substitution of the numerical values:

$$\frac{\lambda_m(Te_2)}{\lambda_m(Te_1)} = \frac{2}{1.738} \left\{ 1 - \left(\frac{1}{2} \right)^{1.738} \right\} = 0.81 \qquad (11)$$

The decrease of Nu for Gr = constant with increase from Te = 0 to Te = 1 is thus theoretically obtained as 19 percent. The previously discussed tests of the four investigators between Gr = 10^{-4} and 10 gave values between 13 percent and 26 percent with a mean value of 22 percent (see fig. 5). This good agreement justifies the assumption of approximately static conducting conditions at small Gr.

II. THEORETICAL SOLUTION OF THE BOUNDARY EQUATIONS FOR THE HORIZONTAL CYLINDER (CASE OF STEADY MOTION)

1. Abstract

The large number of experimental investigations of heat transfer in free convection correspond to only a single physically satisfactory theoretical solution of the differential equations, namely the solution for the vertical plate (two-dimensional steady-flow case) for moderate temperature differences, which was given by Schmidt and Beckmann (ref. 21) with the help of Pohlhausen. The solution is based on the approximation of the Prandtl boundary-layer theory (laminar flow in a layer which is thin as compared with the distance from the lower edge; velocity normal to the wall small as compared with that in the direction of the principal flow along the wall). The results of the theory as regards the velocity and temperature fields and therefore the heat transfer agree very well with the corresponding measurements.

For the case of the horizontal cylinder, schlieren photographs in air (see ref. 22 and figs. 23 and 25) show that, for Grashof characteristics ($Gr = d^3 g\beta\theta/\nu^2$) of about 10^4 and above, the heating of the air extends to only a relatively thin layer around the cylinder, a fact which permits the mathematical simplification of the problem. On the assumption that the heat-transfer and the flow processes are restricted to a thin film, as compared with the cylinder diameter, with laminar flow (boundary-layer assumption) the differential equations (ref. 23) for moderate temperature differences can be solved approximately for the velocity and temperature fields; and therefore the heat transfer can be computed which, in the range of Gr 10^4 to 3×10^8, within which the initial assumptions are satisfied, is in good agreement with experiment.

2. Setting up of Differential Equations

To start, the hydrodynamic differential equations are used in a form previously given (ref. 1)[21] which shows a "lift term", characterizing the free convection, that arises from the combining of the gravity term and the hydrostatic component of the pressure drop, so that only the gradient of the dynamic pressure p^* remains as the pressure force. This dynamic pressure is equal to zero where there is no motion and no temperature difference with respect to the medium at a large distance. As was indicated in detail in reference 1 (p. 429), the density and other characteristics of the substance in the entire field may be considered as constant (case of small temperature difference) and the equations will continue to describe the free-convection problem. The equations in vector form are then[22]

$$\left.\begin{aligned} w^{o}\ \mathrm{grad}\ w &= -1/\rho\ \mathrm{grad}\ p^* - \nu\ \mathrm{rot\ rot}\ w - g\beta\theta \\ \mathrm{div}\ w &= 0 \\ w^{o}\ \mathrm{grad}\ \theta &= a\,\Delta\,\theta \end{aligned}\right\} \qquad (12)$$

with the boundary conditions: $w = 0$, $\theta = \Theta$ on the cylinder surface; and $w = 0$, $\theta = 0$, $p^* = 0$ at infinity. (w, velocity; θ, temperature difference with respect to temperature at infinity; p^*, dynamic pressure; ρ, density; ν, kinematic viscosity; β, expansion coefficient; α, temperature conductivity; $\bar{g}$, gravity acceleration vector; g, its absolute value; r, cylinder radius.)

---

[21] In equation (3c) in reference 1 a minus sign mistakenly appears on the right side.

[22] In place of Δw the invariant form is written grad div w - rot rot w.

For treating the two-dimensional flow about the cylinder, these equations are conveniently written in arc length coordinates with the arc length s on the cylinder perimeter (taken in clockwise direction with the lower stagnation point as origin) and the normal distance n from the cylinder surface, and the velocity components u and v parallel and normal to the wall, respectively. There is then obtained, without neglecting any terms[23]:

$$\underset{1\cdot 1}{\frac{r}{r+n}\,u\,\frac{\partial u}{\partial s}} + \underset{\varepsilon\cdot 1/\varepsilon}{\nu\,\frac{\partial u}{\partial n}} + \underset{1\cdot\varepsilon}{\frac{u\cdot v}{r+n}} = -\frac{1}{\rho}\frac{\partial p^*}{\partial s}\frac{r}{r+n} + g\beta\theta\,\sin\frac{s}{r} +$$

$$\underset{\varepsilon^2\ 1/\varepsilon^2}{\nu\left\{\frac{\partial^2 u}{\partial n^2}\right.} + \underset{1/\varepsilon}{\frac{1}{r+n}\,\frac{\partial u}{\partial n}} + \underset{1}{\frac{r^2}{(r+n)^2}\,\frac{\partial^2 u}{\partial s^2}} - \underset{1}{\frac{u}{(r+n)^2}} + \underset{2\ \cdot\ \varepsilon}{\left.\frac{2r}{(r+n)^2}\,\frac{\partial v}{\partial s}\right\}}$$

$$\underset{1\cdot\varepsilon}{\frac{r}{r+n}\,u\,\frac{\partial v}{\partial s}} + \underset{\varepsilon\cdot 1}{v\,\frac{\partial v}{\partial n}} - \underset{1}{\frac{u^2}{r+n}} = -\frac{1}{\rho}\frac{\partial p^*}{\partial n} - g\beta\theta\,\cos\frac{s}{r} +$$

$$\underset{\varepsilon^2\ 1/\varepsilon}{\nu\left\{\frac{\partial^2 v}{\partial n^2}\right.} + \underset{1}{\frac{1}{r+n}\,\frac{\partial v}{\partial n}} + \underset{\varepsilon}{\frac{r^2}{(r+n)^2}\,\frac{\partial^2 v}{\partial s^2}} - \underset{\varepsilon}{\frac{v}{(r+n)^2}} - \underset{2\ \cdot\ 1}{\left.\frac{2r}{(r+n)^2}\,\frac{\partial u}{\partial s}\right\}}$$

$$\underset{1}{\frac{r}{r+n}\,\frac{\partial u}{\partial s}} + \underset{1}{\frac{\partial v}{\partial n}} + \underset{\varepsilon}{\frac{v}{r+n}} = 0 \qquad (13)$$

$$\underset{1\cdot 1}{\frac{r}{r+n}\,u\,\frac{\partial \theta}{\partial s}} + \underset{\varepsilon\cdot 1/\varepsilon}{v\,\frac{\partial \theta}{\partial n}} = a\left\{\underset{\varepsilon^2\ 1/\varepsilon^2}{\frac{\partial^2\theta}{\partial n^2}} + \underset{1/\varepsilon}{\frac{1}{r+n}\,\frac{\partial \theta}{\partial n}} + \underset{1}{\frac{r^2}{(r+n)^2}\,\frac{\partial^2\theta}{\partial s^2}}\right\}.$$

The approximations made according to the boundary-layer theory are now introduced. The cylinder radius r and hence also s (with the exception of the lower stagnation point) and u are assumed to be of the order of magnitude 1; n is assumed to be of the order of magnitude of

[23] The hydrodynamic equations agree, except for the dynamic pressure and lift terms, with the equations (10), (11), and (12) for r = constant of W. Tollmien: in Wien-Harms, Handb. d. Exp. Phys., IV, 1, p. 248.

the boundary-layer thickness $\varepsilon \ll 1$, so that $n + r$ may be replaced by r. The estimate of the order of magnitude of the individual terms according to the method given by Prandtl and his coworkers then gives the results written underneath the individual terms. In order that the friction and inertia forces may be of equal effect, it is necessary that ν (and correspondingly α) be of the order of magnitude of ε^2. In order that the lift forces for the motion in the direction of the main stream be of significance as compared with the inertia and friction forces, that is, in order that 'free convection' exist at all, it is necessary that $g\beta\theta \approx 1$. From the two momentum equations it then follows that the pressure terms are at most ≈ 1. Since p^* is zero at the outer edge of the boundary layer, it follows from

$$\frac{1}{\rho}\frac{\partial p^*}{\partial n} \approx 1$$

by integration from the outer edge of the boundary layer to the cylinder surface over the length ε that p^*/ρ in the boundary layer can at most be of the order of magnitude ε, that is, so that $1/\rho\ \partial p^*/\partial s = \varepsilon$.

Since in what follows only the terms of the order 1 are retained, the following result, important for simplifying the mathematical treatment, is obtained: The tangential drop of the dynamic pressure is to be neglected as compared with the tangential lift, inertia, and friction forces. The term p^* alone is contained in the equation of the normal momentum. Hence, u, v, and θ are to be computed from the equation of the tangential momentum, the continuity equation, and the heat-transfer equation (eq. (14)). Thereafter p^* may, if desired, be computed from equation (15) of the normal momentum. Hence, the boundary-layer equations for the horizontal cylinder for free convection are

$$\left.\begin{aligned} u\frac{\partial u}{\partial s} + v\frac{\partial u}{\partial n} &= \nu\frac{\partial^2 u}{\partial n^2} + g\beta\theta \sin\frac{s}{r} \\ \frac{\partial u}{\partial s} + \frac{\partial v}{\partial n} &= 0 \\ u\frac{\partial \theta}{\partial s} + v\frac{\partial \theta}{\partial n} &= a\frac{\partial^2 \theta}{\partial n^2} \end{aligned}\right\} \qquad (14)$$

$$-\frac{u^2}{r} = -\frac{1}{\rho}\frac{\partial p^*}{\partial n} - g\beta\theta \cos\frac{s}{r} \qquad (15)$$

A corresponding estimate of equations (13), first rendered nondimensional, gives the two corresponding conditions:

$$\frac{1}{Re} \approx \varepsilon^2 \text{ and } \frac{Gr}{Re^2} \approx 1, \text{ i.e. } Gr \approx \frac{1}{\varepsilon^4} \qquad (b)$$

For a maximum ε, in the sense of the approximations, of 0.1 (approximation to about 10 percent), this gives $Re = 100$ and $Gr = 10^4$ as lower limits of the computations. The approximation is therefore better the larger Gr, that is, the smaller the boundary-layer thickness ε. The upper limit is then attained if the boundary layer becomes turbulent, which (according to part IV) is the case for $Gr = 3.5 \times 10^8$ at the upper stagnation point, for $Gr = 3 \times 10^9$ at the equator. The range of applicability of the laminar-boundary-layer computations therefore lies between $Gr = 10^4$ and $Gr = 10^9$.

3. Reduction to Ordinary Differential Equations

The usual introduction of the stream function Ψ

$$u = \frac{\partial \Psi}{\partial n} \qquad v = -\frac{\partial \Psi}{\partial s} \qquad (16)$$

eliminates the continuity equation. By introducing nondimensional magnitudes with $Gr' = r^3 g\beta\theta/\nu^2$ by means of the transformation[24]:

$$x = \frac{s}{r} \qquad y = \frac{n}{r} Gr'^{1/4} \qquad \Psi = \frac{\Psi}{\nu} Gr'^{-1/4} \qquad \tau = \frac{\theta}{\Theta} \qquad (17)$$

there remain of the five constants (ν, $g\beta$, α; θ, r) of differential equations (14) only two in the nondimensional combination of the Prandtl characteristic $Pr = \nu/\alpha$.

$$\frac{\partial \Psi}{\partial y}\frac{\partial^2 \Psi}{\partial x\, \partial y} - \frac{\partial \Psi}{\partial x}\frac{\partial^2 \Psi}{\partial y^2} - \frac{\partial^3 \Psi}{\partial y^3} + \tau \sin x$$

$$\frac{\partial \Psi}{\partial y}\frac{\partial \tau}{\partial x} - \frac{\partial \Psi}{\partial x}\frac{\partial \tau}{\partial y} = \frac{1}{Pr}\frac{\partial^2 \tau}{\partial y^2} \qquad (18)$$

Equation (17) is not an arbitrary transformation which carries equation (14) over into equation (18), but a definitely determined transformation with the aid of which it is possible to eliminate Gr

---

[24] Gr' referred to r is more convenient for the computation than Gr referred to d. In the final result, the more usual Gr is again introduced.

so that it no longer occurs in equation (18). The solution of equation (18) therefore likewise no longer contains Gr. It is therefore unnecessary to know the solution of equation (18) if it is of interest to know only how the solution (e.g., velocity, temperature, boundary-layer thickness, heat-transfer coefficient) of the initial equation (14) depends on the Gr number. This dependence of Gr is already completely represented by the transformation (17), whereas equation (18) contains the further dependence on Pr and on the space coordinates. In other words, the solution of equation (18), obtained for a definite Pr value[24a] gives, by means of equation (17), at the same time the velocity and temperature fields for all Gr values. On the other hand, the transformation (17) without the solution of equation (18) already gives important general information on the flow condition and the heat transfer for free convection with respect to the dependence on Gr. From equation (17) there follows, if the following expression is set up,

$$U = \frac{\partial \Psi}{\partial y} \qquad V = -\frac{\partial \Psi}{\partial x} \tag{19}$$

that

$$\frac{n}{r} = y\,Gr'^{-1/4} \qquad \frac{ur}{\nu} = U\,Gr'^{1/2} \qquad \frac{vr}{\nu} = V\,Gr'^{1/2} \qquad \frac{r}{\theta}\frac{\partial \theta}{\partial n} = \frac{\partial \tau}{\partial y}\,Gr'^{1/4} \tag{20}$$

That is, the relative boundary-layer thicknesses decrease with $Gr^{-1/4}$; the nondimensional velocities increase with $Gr^{1/2}$; and the nondimensional temperature drop increases with $Gr^{1/4}$, from which there follows directly the well-known 1/4-power law of heat transfer in free convection:

$$Nu \sim Gr^{1/4} \tag{21}$$

These theoretical results agree with those for the rectangular plate and are not restricted to the latter and the horizontal cylinder alone, but depend on more general assumptions (ref. 19). They are valid, in general, for all two-dimensional cases of free flow with a boundary-layer character (ref. 23), that is, where the thickness of the heated laminar layer is small compared with the distance from the incidence edge and the radius of curvature of the wall, and the latter does not change discontinuously in the flow direction. The existence of sharp edges about which the flow occurs is therefore excluded. In this more general case, there are on the right side of equation (13) additional terms which are determined by the radius of curvature and which

[24a] It is here assumed as self evident from physical considerations that one and one only such solution exists. On the mathematical side of these existence and uniqueness proofs, see the discussion in reference 1 (p. 428).

vary with the arc length $(\partial r/\partial s)$ but which drop out in the estimate made under the initial assumptions. Furthermore, in place of the sine and cosine of the lift term there appear functions which determine the direction of the surface element with respect to the horizontal and vertical but which similarly do not change anything in the transformations (17) and the conclusions from equations (20) and (21) based on these transformations.

In agreement with these theoretical conclusions equation (21) has already been confirmed for vertical plates (ref. 21), horizontal cylinders[25], and cylindrical layers (ref. 24), and even for the heat transfer from the two sides of a square horizontal thick plate with edges (ref. 25) and for the heat transfer with evaporation at a vertical cylinder in water and carbon tetrachloride (ref. 26) for which the previously mentioned assumptions are not all satisfied.

A reduction of the partial differential system (18) to systems of ordinary differential equations is attempted by setting

$$q = y\, g(x) \tag{22a}$$

$$\Psi(x,y) = p(q)f(x) \tag{22b}$$

$$\tau(x,y) = t(q) \tag{22c}$$

for example,

$$U = \frac{\partial \Psi}{\partial y} = f(x)g(x)p'(q) \tag{22d}$$

based on the notion that all the profiles of the stream function $\psi(y)$, tangential velocity $U(y)$, and temperature $\tau(y)$ for the different azimuths x of the cylinder are produced by affine distortions by means of the azimuth functions $f(x)$ and $g(x)$ from a single "base profile" of the stream function $p(q)$ or the velocity $p'(q)$ and one base profile of the temperature $t(q)$ (q = normal coordinate of the base profile). Substitution of equation (22) in equation (18) gives (primes of p and t denote differentiation with respect to q; primes of f and g denote differentiation with respect to x):

$$\left.\begin{aligned} p'^2(f^2gg' + ff'g^2) - pp''ff'g^2 &= p'''fg^3 + t \sin x \\ 1/Pr\ gt'' + f'pt' &= 0 \end{aligned}\right\} \tag{23}$$

[25]See Part I, section 5, figure 10.

A separation into functions of the two independent variables x and q, that is, a successful application of the assumed expression (eq. (22)) for solving the equations, is possible only if the two functions $f(x)$ and $g(x)$ can be uniquely determined from the four ordinary differential equations

$$f'(x) = ag(x) \tag{24a}$$

$$f(x)f'(x)g^2(x) = c \sin x \tag{24b}$$

$$f^2(x)g(x)g'(x) = b \sin x \tag{24c}$$

$$f(x)g^3(x) = d \sin x \tag{24d}$$

(where a,b,c,d are initially undetermined constants) in spite of the redundancy of the equations[26]. The possibility of such unique determination, which is the necessary assumption for the applicability of equation (22), will be discussed in more detail after equation (29) is considered. If such determination is possible, there remain for $p(q)$ and $t(q)$ two ordinary differential equations:

$$\left.\begin{aligned}(b + c)p'^2(q) - cp(q)p''(q) &= dp'''(q) + t(q)\\ t''(q) + a\,\mathrm{Pr}\,p(q)t'(q) &= 0\end{aligned}\right\} \tag{25}$$

In section 4, equation (24) will be solved and in section 5 equation (25) will be discussed.

4. Determination of the Azimuth Functions $F(x)$ and $G(x)$

(a) Setting up of the two differential equations for $F(x)$. - The boundary values of $f(x)$ and $g(x)$ which are required for solving equation (24) are determined from physical considerations. From

$$\frac{\partial \tau}{\partial y} = \frac{dt(q)}{dq}\, g(x)$$

it follows that

$$g(x = 0) = g_0 \neq 0 \tag{26a}$$

[26]The author is indebted to Dr. A. Naumann, Leipzig, for several mathematical suggestions.

Otherwise, the temperature of the cylinder surface would also be the temperature in the field along the entire normal at the lower stagnation point, which cannot be the case. From equation (24a) there is then obtained

$$f'(x = 0) = ag_0 \tag{26b}$$

Since the tangential velocity at the lower stagnation point must, for reasons of symmetry, be different, there follows from equation (22d):

$$f(x = 0) = 0 \tag{26c}$$

The system of equation (24) with the boundary conditions (26a), (26b), and (26c) thus contains five free available constants a,b,c,d, and g_0, which are determined in subsequent computation.

By introducing the normed functions[27]:

$$F(x) = \frac{f(x)}{ag_0} \qquad G(x) = \frac{g(x)}{g_0} \tag{27}$$

equation (24) may be transformed to:

$$F' = G \tag{28a}$$

$$F^2 G G' = \frac{b}{a^2 g_0^4} \sin x \tag{28b}$$

$$F F' G^2 = \frac{c}{a^2 g_0^4} \sin x \tag{28c}$$

$$F G^3 = \frac{d}{a g_0^4} \sin x \tag{28d}$$

with the boundary conditions

$$F(x = 0) = 0 \qquad F'(x = 0) = 1 \qquad G(x = 0) = 1 \tag{29}$$

A necessary assumption for the applicability of the expressions of equation (22) for solving the equations is that the two functions F and G can be uniquely determined from the four equations (28a) to (28d). This would be the case if it could be proven that the four

[27]By normed is meant fully determined also with respect to a factor.

equations are not independent of one another, but that two equations follow from the other two. This proof is partly possible only insofar as one equation (for suitable choice of the constants) is a consequence of the remaining equations. Thus, elimination of G with the aid of equation (28a) gives

$$F^2 F' F'' = \frac{b}{a^2 g_0^4} \sin x \tag{30a}$$

$$F F'^3 = \frac{c}{a^2 g_0^4} \sin x \tag{30b}$$

$$F F'^3 = \frac{d}{a g_0^4} \sin x \tag{30c}$$

Equation (30c) is thus a consequence of equation (30b) in the case that the following first condition for the constants is satisfied:

$$d = c/a \tag{31}$$

Setting for briefness

$$c/a^2 g_0^4 = \alpha \tag{32a}$$

$$b/a^2 g_0^4 = \beta \tag{32b}$$

there then remain for the determination of F the two equations

$$F F'^3 = \alpha \sin x \tag{33I}$$

$$F^2 F' F'' = \beta \sin x \tag{33II}$$

with freely available values of α and β. As a necessary assumption for the applicability of equation (22), there remains the further condition that the two equations I and II possess two equal (or at least approximately equal) solutions.

This proof will be obtained by solving equations I and II by a power-series development above and below the equator $x = \pi/2$. For this purpose, with $\varphi = x - \pi/2$, I and II are transformed into

$$F(\varphi)F'^3(\varphi) = \alpha \cos \varphi \tag{34I}$$

$$F^2(\varphi)F'(\varphi)F''(\varphi) = \beta \cos \varphi \tag{34II}$$

where the primes now denote differentiation with respect to φ.

(b) Solution of differential equation (I) for F. - The value of α, by the boundary values of equation (29), is first determined as

$$\alpha = 1 \tag{32c}$$

as is seen from the first term of the power-series development of equation (33I) about the point $x = 0$. From the expression for solving equation (34I):

$$F^I(\varphi) = a_0(1 + c_1 \varphi + c_2 \varphi^2 + \ldots) \tag{35}$$

there follows

$$F^I(\varphi = 0) = a_0 \qquad F^{I'}(\varphi = 0) = a_0 c_1 \tag{36a}$$

and by substituting in equation (34I)

$$a_0^4 c_1^3 = \alpha = 1 \tag{36b}$$

Substitution of expression (35) in differential equation (34I) gives the unknown coefficients, which are taken up to the fifth, inclusive, and which can be successively determined in terms of c_1:

$$\left.\begin{aligned} c_2 = -\frac{1}{6} c_1^2 \qquad c_3 = -\frac{1}{18} c_1 + \frac{5}{54} c_1^3 \qquad c_4 = \frac{1}{54} c_1^2 - \frac{5}{72} c_1^4 \\ c_5 = -\frac{1}{360} c_1 - \frac{5}{324} c_1^3 + \frac{13}{216} c_1^5 \end{aligned}\right\} \tag{37}$$

The boundary condition $F^I(\varphi = -\pi/2) = 0$ according to equation (29) gives for the value of c_1 the solution of an algebraic equation of the fifth degree which is solved by trial

$$c_1 = 0.581 \tag{38}$$

Of the five possible real roots it is necessary to choose that one for which no further zero of F^I is obtained between $\varphi = 0$ and $\varphi = -\pi/2$. The coefficients then assume, according to equation (37), the values

$$\left.\begin{aligned} c_1 = +0.581 \qquad c_2 = -0.05626 \qquad c_3 = -0.01412 \\ c_4 = -0.00165 \qquad c_5 = -0.00066 \end{aligned}\right\} \tag{39}$$

According to equations (36a), and (36b), there is obtained

$$F^I(\varphi = 0) = a_0 = 1.504 \qquad F^{I'}(\varphi = 0) = a_0 c_1 = 0.874 \tag{40}$$

and the numerical solution of $F^{I}(\varphi)$ is thereby completely given (see table III).

It may be remarked[27a] that for equation (33I) a solution was also obtained by a power-series expansion at the point $x = 0$ in powers of $\sin(x/2)$ which, because of the fact that the curvature of F at that point is zero, converges with particular rapidity:

$$F^{*}(x) = 2 \sin \frac{x}{2} \left(1 + \frac{1}{10} \sin^2 \frac{x}{2} + \frac{4}{100} \sin^4 \frac{x}{2} + \ldots\right) \qquad (41)$$

This solution assumes at the equator the values

$$F^{*}(x = \pi/2) = 1.500 \qquad F^{*\prime}(x = \pi/2) = 0.874 \qquad (e)$$

which are in good agreement with the values of equation (40) of the series expansion at the equator. In this way, the sufficient convergence of $F^{I}(\varphi)$ with the five computed terms is assured, and a good check is obtained against computation errors. The solution F^{*} will not be used in what follows; this is because of the singular behavior of equation (33II) at the point $x = 0$, and the identity proof must therefore be carried out by the series expansion at the equator.

(c) Solution of differential equation II for F. - For equation (34II), corresponding to equation (35), the following expression is assumed:

$$F^{II}(\varphi) = b_0(1 + d_1\varphi + d_2\varphi^2 + \ldots) \qquad (42)$$

Substitution in the differential equation gives the following values for the constants: b_0 and d_1 are arbitrary

$$\left.\begin{aligned} d_2 &= \frac{\beta}{2b_0{}^4 d_1} \\ d_1\, d_3 &= -\frac{2}{3}\left(d_1{}^2 d_2 + d_2{}^2\right) \end{aligned}\right\} \qquad (43)$$

where, on account of the length of the expressions, d_4 and d_5 are not given as functions of d_1 and d_2. The function F^{II} thus depends

[27a]Acknowledgment is made to Prof. W. Müller, Aachen, for the suggestion that the solution of equation (33I) may be reduced to two quadratures by separation of the variables. One of the quadratures is not in closed form, however, but can be carried out only by a series expansion so that this method would not be essentially different from the one employed.

on the as yet freely available values of b_0, d_1, and β. The solutions F^I and F^{II} are equal if the corresponding coefficients of the series are equal. Therefore, the as yet undetermined coefficients are equated as follows:

$$b_0 = a_0 \qquad d_1 = c_1 \tag{44}$$

The condition $d_2 = c_2$ gives

$$\frac{\beta}{2b_0{}^4 d_1} = -\frac{1}{6} c_1{}^2 \tag{f}$$

or with equations (36b) and (44)

$$\beta = -1/3\ \alpha = -1/3 \tag{45}$$

All the coefficients may now be expressed in terms of d_1:

$$d_2 = -\frac{1}{6} d_1{}^2 \qquad d_3 = +\frac{5}{54} d_1{}^3 \qquad d_4 = +\frac{1}{72} d_1{}^2 - \frac{5}{72} d_1{}^4$$

$$d_5 = -\frac{7}{540} d_1{}^3 + \frac{13}{216} d_1{}^5 \tag{46}$$

Comparison of the coefficients of the two series for F^I and F^{II} gives

$$b_0 - a_0 \equiv 0 \qquad d_1 - c_1 \equiv 0 \qquad d_2 - c_2 \equiv 0 \qquad d_3 - c_3 = \frac{1}{18} c_1$$

$$d_4 - c_4 = -\frac{1}{216} c_1{}^2 \qquad d_5 - c_5 = +\frac{1}{360} c_1 + \frac{1}{405} c_1{}^3 \tag{47}$$

This result states that the solutions of the two different differential equations (34I) and (34II) agree at the equator in the value of the function, in the tangent, and in the curvature, but not in the higher derivatives in which they differ fundamentally to a small degree. F^I and F^{II} are approximately, but not rigorously, equal. The system (24) is, strictly speaking, overdetermined and has only approximately unique solution. This solution of expression (22) is not rigorously, but only approximately, valid. Because of the agreement of F^I and F^{II} at the equator up to and including the curvature, however, these differences become more appreciable in the neighborhood of the lower and upper stagnation points where the initially assumed boundary-layer assumptions are not satisfied. The method that has here been employed thus gives an approximate solution of the boundary-layer equations within the accuracy limits determined by the physical approximations of the boundary-layer assumptions.

The numerical computation of equations (44) and (46) with a_0 and c_1 according to equations (40) and (39) gives:

$$b_0 = 1.504 \quad d_1 = 0.581 \quad d_2 = -0.05626 \quad d_3 = +0.01816$$

$$d_4 = -0.00321 \quad d_5 = +0.00144 \qquad (48)$$

Table III shows the values of the functions $F^I(\varphi)$ and $F^{II}(\varphi)$ computed according to equations (39), (40), and (48), with sufficient agreement between $x = 30^o$, 150^o and even at 165^o (graphically interpolated for F^{II}). The negative value of F^{II} for $x = 0$ has no significance since, on account of the singular behavior of equation (34II) for $F = 0$, the series (42) beyond this singular point no longer represents the solution of the differential equation. For the further equations, F^I is employed because only this function possesses the required property of vanishing at the lower stagnation point.

(d) Determination of G. - The term G is determined according to equation (28d) where, according to equation (49), $d = ag_0^4$. Table III shows the computed values based on F^I.

5. Determination of Basic Profiles p(q) and t(q)

The constants b, c, d which occur in equation (25) can now, with the aid of equations (31), (32a), to (32c), and (45) be expressed in terms of a and g_0:

$$b = -1/3\, a^2 g_0^4 \quad c = a^2 g_0^4 \quad d = a g_0^4 \qquad (49)$$

Equation (25) then becomes

$$\left.\begin{aligned} 2/3\, a^2 g_0^4 p'^2 - a^2 g_0^4 p p'' &= a g_0^4 p''' + t \\ t'' + a \,\mathrm{Pr}\, p t' &= 0 \end{aligned}\right\} \qquad (50)$$

with the boundary conditions:

$$q = 0: \; p = 0 \quad p' = 0 \quad t = 1$$

$$q = \infty: \; p' = 0 \quad t = 0 \qquad (g)$$

Equation (50) for $a = 1$ and $g_0 = 1$ may now be numerically integrated. The following values were chosen for the as yet free remaining constants a and g_0

$$a = 3 \qquad g_0 = 3^{-1/4} \tag{51}$$

equation (50) becomes

$$\left.\begin{aligned} p''' + 3\,p\,p'' - 2\,p'^2 + t = 0 \\ t'' + 3\,Pr\,p\,t' = 0 \end{aligned}\right\} \tag{52}$$

This system with the same boundary conditions and for $Pr = 0.733$ (diatomic gases) has already previously been numerically integrated by E. Pohlhausen for the vertical plate so that, because of the introduction of the normed functions F and G and the consequent availability of the constants, a new numerical integration is unnecessary. The stream function $p(q)$ and temperature function $t(q)$ correspond to the functions $\zeta(\xi)$ and $\theta(\xi)$ of Pohlhausen. Their values are given in reference 21 in tabular form (ref. 4, p. 187). Graphical representations of the velocity profile $p'(q)$ and of the temperature profile $t(q)$ are given in figures 13 to 16 (continuous curves).

6. Complete Solution for Velocity and Temperature Fields

With the values of equations (51) for a and g_0, the azimuth functions $f(x)$ and $g(x)$ according to equation (27) are now uniquely determined. For

$$a\,g_0 = 3^{3/4} = 2.280 \qquad g_0 = 3^{-1/4} = 0.760 \tag{53}$$

there is obtained

$$f(x) = 2.280\,F(x) \qquad g(x) = 0.760\,G(x) \tag{54}$$

Table IV shows the values of $f(x)$, $g(x)$, and $f(x)\cdot g(x)$ computed from F^I and G of table III. Figure 17 shows these values graphically.

With the values $f(x)$ and $g(x)$ from table IV, the values $p(q)$ and $t(q)$ from the table of Pohlhausen and the transformations (16), (17), and (22) there is obtained the complete solution of the boundary-layer equations (14) for the velocity (u and v) and temperature fields (θ) obtained without any empirical value. Collecting results yields (see also eq. (19) and (20) for simultaneous passage from Gr' to Gr ($Gr = 8Gr'$):

$$u(s,n) = \frac{\nu}{r}\frac{Gr^{1/2}}{8^{1/2}} f(x)g(x)\, p'(q)$$

$$v(s,n) = -\frac{\nu}{r}\frac{Gr^{1/4}}{8^{1/4}}\left\{f'(x)p(q) + \frac{f(x)g'(x)}{g(x)}\, q\, p'(q)\right\} \qquad (55a\text{-}55d)$$

$$\theta(s,n) = \Theta t(q) \qquad \frac{\partial\theta}{\partial n}(s,n) = \frac{\Theta}{r}\frac{Gr^{1/4}}{8^{1/4}} g(x)t'(q)$$

$$\text{with } x = \frac{s}{r} \text{ and } q = \frac{n}{r}\frac{Gr^{1/4}}{8^{1/4}} g(x)$$

For the determination of the normal velocity v it is required to know $f'(x)$ and $g'(x)$. The term $f'(x)$ is, according to equation (24), determined by means of $g(x)$; $g'(x)$ was determined by graphical differentiation of $g(x)$[28]. Here the qualitative description of the normal velocity obtained from the streamline picture is sufficient. It can be shown that the boundary conditions of u, v, θ for $q = 0$ are correctly assumed. If the assumption $n \ll r$ which was made with respect to the solution of equation (14) is applied for very large q, there are obtained for u and θ the correct value zero; but for v, in contradiction to the boundary conditions (12), a finite value is obtained which is related to the fact that the cylinder curvature was neglected.

The boundary-layer thickness, tangential velocity, temperature, and heat-transfer coefficients according to equation (55) behave as follows. With regard to the dependence of these magnitudes on Gr, there hold first of all the considerations of section 3 in connection with equations (20) and (21). The dependence on the cylinder azimuth is such that all profiles of the tangential velocity and temperature are obtained by affine distortions from the basic profiles $p'(q)$ and $t(q)$.

The value $1/g(x)$ (fig. 17) represents the 'extension' of the temperature and velocity profiles normal to the surface with increasing azimuth, that is, the development of any characteristic distance from the wall, for example, of the place of maximum velocity ($q = 0.95$) or of the boundary-layer thickness to be defined later ($q = 2.18$). In accordance with this, the boundary-layer thickness at the lower stagnation point possesses a finite approximately constant value over a

[28]The values are not given here.

large azimuth range but increases at first gradually then more and more rapidly and attains at the upper stagnation point a theoretically infinitely large value (upward current of warm air). The function $g(x)$, since it is proportional to the temperature drop, likewise represents the variation of the local heat-transfer coefficient with the cylinder azimuth. At the lower stagnation point, $g(x)$ is constant and with constant slope connects with the values of the other side of the cylinder. At the upper stagnation point ($x = \pi$) this is no longer the case; $g(x)$ has a sharp peak which is associated with the fact that the boundary-layer assumptions at this point strongly deviate from the actual conditions (normal velocity large as compared with the tangential velocity). Under actual conditions this peak is balanced out by a very sharp minimum value as is shown by the value of Nu along the cylinder perimeter computed from the schlieren pictures of E. Schmidt (ref. 22)[29]. No quantitative comparison of this experimental curve of $g(x)$ with the theoretical curve given herein can be given because the conditions of the two-dimensional problem are so little satisfied for the schlieren pictures (pipe length = 2 times cylinder diam.) that the computed heat-transfer coefficient is 40 percent greater than that of the tests of Koch (ref. 22).

The development of the tangential velocity with the azimuth, that is, the increase of any characterizing velocity, for example the maximum velocity, is described by $f(x) \cdot g(x)$ (see fig. 17). The velocity increases from the value zero at the lower stagnation point (up to 60° approximately linearly) to a maximum at about 128° and, on approaching the upper stagnation point (convergence of the flow on either side) rapidly decreases to zero. This physically correct behavior of the solution at the upper stagnation point is not introduced as a boundary condition but is obtained as a necessary consequence of the theory.

An over-all picture of the velocity and temperature fields is given by the streamlines and isotherms (figs. 11 and 12). They are computed from the equations

$$\left.\begin{aligned} \frac{\psi(x,n/r)}{\nu} &= f(x)Gr'^{1/4}\, p\left[\frac{n}{r} Gr'^{1/4}\, g(x)\right] = \text{const} \\ \frac{\theta(x,n/r)}{\Theta} &= t\left[\frac{n}{r} Gr'^{1/4}\, g(x)\right] = \text{const} \end{aligned}\right\} \quad (55e,f)$$

for various values of the constants[30]. The scale of the representation

[29]See figure 13 for maximum $Gr = 16 \times 10^6$.

[30]The streamline picture for azimuth intervals of 15° and in addition for 5°, 10°, 170°, 175°; the isotherm picture for azimuth intervals of 30° and in addition for 165°, 170°, 175°.

holds for $Gr = 10^4$; for $Gr = 10^6$ the distances from the cylinder surface should be reduced by a factor of 3.16 and for $Gr = 10^8$, by 10. At the lower and equatorial neighborhood of the cylinder up to an azimuth of about 105°, the flow near the wall is directed toward the surface, while above it is directed away from the surface upwards. In this respect the theoretical solution for the cylinder differs fundamentally from that for the vertical plate, which gives only a flow toward the plate. The isotherms at the lower part form almost concentric circles. At the upper stagnation point (upward warm current) the isotherms theoretically go toward infinity, whereas actually (corresponding to the gradual dissolution and spreading out of the warm upstreaming air) they close at a relatively large distance over the cylinder. The isotherm 0.53 gives at the same time the place of the maximum tangential velocity.

7. Heat-Transfer Law

From the expression for the quantity of heat dQ passing from an element of area df,

$$dQ = \lambda \left(- \frac{\partial \theta}{\partial n} [n = 0] \right) df \tag{56}$$

the value of the temperature gradient at the wall obtained from equation (55c)

$$\frac{\partial \theta}{\partial n} (n = 0) = \frac{\Theta}{r} Gr'^{1/4} g(x) t'_0 \tag{57}$$

($t'_0 = t'(q = 0) = -0.508$), and the defining equation for locally variable heat-transfer coefficient $a(x)$

$$\alpha(x) = \frac{1}{\Theta} \frac{dQ}{df} \tag{58}$$

there is obtained

$$\frac{\alpha(x) \cdot r}{\lambda} = g(x)(-t_0') Gr'^{1/4} \tag{59}$$

From this there is obtained for the dependence of the nondimensional local heat-transfer coefficient on the cylinder azimuth x and the Gr number ($Gr_d = 8Gr'$)[30a]:

[30a] Since several formulas of this section will be used later in Part III, and in order to avoid misunderstandings, indices (e.g., d,h,H) for the characteristics Gr and Nu are written which indicate the lengths with which these magnitudes are formed.

$$\frac{\alpha(x) \cdot d}{\lambda} = Nu_d(x) = 0.604\ g(x)\ Gr_d^{1/4} \tag{60}$$

see figure 18.

To compute the mean heat-transfer coefficient averaged over the cylinder perimeter,

$$\alpha_m = \frac{1}{\pi} \int_0^{\pi} \alpha(x)\ dx \tag{61}$$

there is required the mean value

$$\bar{g} = \frac{1}{\pi} \int_0^{\pi} g(x)\ dx \tag{62}$$

which, by planimetering $g(x)$ (fig. 17), is found to be

$$\bar{g} = 0.616 \tag{63}$$

It may also be computed by the following relation from equation (24a) with $a = 3$ according to equation (51)

$$3\ \pi\ \bar{g} = f(\pi) \tag{64}$$

which gives $\bar{g} = 0.620$. However, the value 0.616 is preferable because this value takes into account the total curve $g(x)$ and does not depend on the end point of the series expansion $f(x)$. From equation (60) the following is then obtained for the mean heat-transfer coefficient as a function of Gr for free flow at a horizontal cylinder

$$\frac{\alpha_m \cdot d}{\lambda} = Nu_d = 0.372\ Gr_d^{1/4} \tag{65}$$

A comparison of this theoretical heat-transfer coefficient for diatomic gases ($Pr = 0.74$) with test results is given in Part I, section 5; see also figure 10.

8. Comparison of Theoretical Velocity and Temperature Fields with Available Measurements

The comparison of the computed velocity and temperature fields is carried out with the measurements of Jodlbauer (ref. 16) which are the

only ones thus far available[31]. Of the fields measured for six different Gr values, the following ones were computed:

$2r = 9$ cm, $t_w = 99.2^\circ$, $t = 18.1^\circ$, $Gr = 3.76 \times 10^6$ (figs. 13, 14)
$2r = 5$ cm, $t_w = 104.6^\circ$, $t = 18.1^\circ$, $Gr = 6.54 \times 10^5$ (figs. 15, 16)

The best agreement with theory is to be expected for the maximum Gr. On the basis of the theory it would be desirable to have measurements for the largest possible laminar Gr, that is (see Part IV) values of about 3.5×10^8, which could be realized in air at 20° C at a surface temperature of 100° C with cylinders of 42 centimeters diameter. 16.53 inches

The comparison with the theory was carried out in such manner that all velocity profiles $u(s,n)$ and temperature profiles $\theta(s,n)$ corresponding to a value of Gr were, with the aid of equation (55), recomputed for the theoretical basic profiles $p'(q)$ and $t(q)$ in the representation of which they must all coincide.

In the case of the velocity profiles (figs. 13 and 14), there is a regular deviation in that the measured velocities are greater than the computed ones, the deviation from the theory in the maximum velocity amounting on the average to 22 percent for the smaller and 17 percent for the larger value of Gr. A part of the deviations occurring for large distances from the wall beyond the maximum value should be ascribed to the uncertainties in the difficult measurements of such small air velocities, as can be seen from the following discrepancies. The measured velocities at the azimuth 60° for $Gr = 3.76 \times 10^6$ lie considerably above the theoretical curve, whereas for $Gr = 6.54 \times 10^5$ they lie on the theoretical curve. On the other hand, the velocities measured at $x = 30^\circ$ for $Gr = 6.54 \times 10^5$ show strong deviations upward, whereas for $Gr = 3.76 \times 10^6$ they are in agreement with the theory. The measured distance from the wall of the maximum value of the velocity is everywhere in very good agreement with the theory.

The measured temperature profiles show very good agreement with the theory even for the azimuth of 165°. A small regular deviation is noted for all azimuths and Gr numbers for medium distances from the wall. The small deviations at small distance from the wall can be ascribed partly to the fact that the condition for the isothermal surface was not quite satisfied in the tests. The measured temperature

---

[31]Acknowledgment is made to Prof. E. Schmidt and Dr. K. Jodelbauer for their aid in providing the data.

drops at the wall for $Gr = 6.54 \times 10^5$ are on the average 3 percent smaller than the values given by the theory, while for $Gr = 3.76 \times 10^6$ they are 1 percent higher[32].

It is likewise of interest to compare the solution based on the boundary-layer theory for the vertical plate with the corresponding test results. Reference 21 (figs. 20 to 23) also shows the velocity fields to have stronger deviations than the temperature fields. For the small plate with smaller deviations, the measured velocities also lie somewhat higher than the theoretical values; but for the larger plate with larger deviations the contrary is true. For the temperature fields, particularly for the large plate, no regular deviation can be established between theory and experiment. The deviations occurring for the plate are clearly smaller in comparison with those for the cylinder. This is to be ascribed to the fact that in the case of the plate only the boundary-layer terms of the order $\varepsilon^2 << 1$ (rectilinear flow) were neglected, whereas for the case of the cylinder there were, in addition, neglected terms of the order $\varepsilon^1 << 1$ that were related to the curvature.

III. HYDRODYNAMIC AND THERMAL COMPARISON BETWEEN VERTICAL PLATE AND HORIZONTAL CYLINDER FOR FREE CONVECTION AND FOR PLATE IN PARALLEL FLOW

1. Abstract

Now that the theoretical boundary-layer solutions for the vertical plate and the horizontal cylinder for free convection have been obtained, it is of advantage to compare these two standard bodies of two-dimensional free flow with regard to the shape of the stream and the heat transfer. Similarly, a comparison of the boundary-layer development between the vertical plate for free convection and for the plate in parallel flow (Blasius solution of the boundary-layer equations) is of interest. The following features are characteristic for the three types of flow.

---

[32]The fact that the values of the heat-transfer coefficient obtained from the field measurements of Jodlbauer through integration of the temperature gradients at the wall over the cylinder perimeter lie, on the average, 4 percent higher than the theoretical values (see fig. 10) is due to the deviation between the theoretical and the actual conditions in the neighborhood of the upper stagnation point.

The boundary-layer thickness of the plate in parallel flow increases with the square root of the distance from the incidence edge; that of the vertical plate in free convection increases, however, as the fourth root of the height above the lower edge (cf. eqs. (69) and (71)). Both start with the thickness zero, which for the plate in parallel flow results in infinitely large velocity gradients, and for the free plate results in an infinitely large temperature drop and an infinitely large local heat-transfer coefficient at the lower edge. In the case of the cylinder, on the contrary, the boundary layer starts at the lower stagnation point of the horizontal cylinder with a finite thickness and thereafter with finite velocity and temperature gradients and a finite local heat-transfer coefficient (fig. 17). It increases according to a complex law ($1/g(x)$, see eqs. (70) and (82)) and at the upper stagnation point reaches a theoretically infinite thickness, with vanishing velocity and temperature drops normal to the surface (upward stream of warm air) and with a vanishing heat-transfer coefficient.

In spite of these fundamental differences it is possible to set up a number of relations between the three cases. These show on the one hand a close hydrodynamic and thermal kinship which is due to the boundary-layer character of the differential equations underlying the theoretical solutions. On the other hand, they give practical viewpoints with regard to the application of rectangular plates or horizontal cylinders for the heat transfer. For this purpose it is first of all necessary to represent the Reynolds numbers of the characteristic length, of the boundary-layer thickness, and of the nondimensional local and average heat-transfer coefficients as functions of the Grashof numbers of the plate and cylinder, which in turn requires the introduction of a boundary-layer thickness (flow discharge thickness) for the velocity profile of the free convection. A knowledge of the dependence of Re of the boundary-layer thickness on Gr of the plate, as well as of the azimuth and Gr of the cylinder, is in addition required for the later evaluation of the tests as regards the occurrence of turbulence (Part IV) for free convection at the plate and the cylinder.

2. Boundary-Layer Thickness for Free Convection

It is first necessary to determine the magnitude to be associated with the boundary-layer thickness. For the velocity profile $u(y)$ of the plate in parallel flow (U = maximum velocity), Prandtl and his coworkers, as is known, introduced the displacement thickness δ^*, defined as

$$\delta^* \cdot U = \int_0^\infty (U - u)\, dy \qquad (66)$$

which is a measure of the decrease in the flow discharge as a result of the friction.

For the velocity profile of the free convection $u(y)$, a flow discharge thickness δ is introduced which is hydrodynamically equivalent to the displacement thickness, being like the latter characteristic of the development of the friction layer, which in this case takes up the entire flow:

$$\delta \cdot U = \int_0^\infty u \, dy \tag{67}$$

or expressed in words: Through the flow discharge thickness δ would flow the same fluid mass with the maximum velocity as actually flows with the total stream.

In the nondimensional velocity profile $p'(q)$ (q = nondimensional distance from the wall, p = stream function) which occurs in the theoretical solution, the discharge flow thickness is denoted by q_δ, the maximum velocity by p'_{max}. From equation (67) there is then obtained:

$$q_\delta p'_{max} = \int_0^\infty p'(q)dq = p(\infty) - p(0)$$

and with the numerical values:

$$p'_{max} = 0.275$$

$$p(\infty) = 0.60^{33}$$

$$p(0) = 0$$

the value of q_δ is obtained as

$$q_\delta = 2.18 \tag{68}$$

For orientation purposes[34], it is assumed that the velocity maximum lies at $q = 0.95$ and the point of inflection of the profile at $q = 1.85$.

With the values of q_δ for the plate and cylinder from equations (72) and (82), respectively, there is obtained for the vertical plate, where h is the distance from the lower edge:

---

[33]Extrapolation from last computed value $p(6.0) = 0.5928$.

[34]See continuous curves in figures 13 and 15.

$$\frac{\delta}{h}\frac{2^{1/2}}{2}\,Gr_h^{1/4} = 2.18 \qquad (69)$$

and for the horizontal cylinder of diameter d at azimuth x

$$\frac{\delta}{d}\,g(x)2^{1/4}\,Gr_d^{1/4} = 2.18 \qquad (70)$$

3. Nondimensional Representation of Theory for Vertical Plate

(a) Reynolds numbers. - From the theoretical solution for the vertical plate given by Schmidt and Pohlhausen (ref. 21) the following expression is obtained according to their equations (23), (24), and (31)[35], since $c^4 = Gr_h/4h^3$, for the velocity u and the distance from the wall y:

$$u = \frac{2\nu}{h}\,p'(q)\,Gr_h^{1/2} \qquad \frac{y}{h} = q\sqrt{2}\,Gr_h^{-1/4} \qquad (71)$$

For the flow discharge thickness $y = \delta$ and the maximum velocity $u = U$, there is then obtained

$$U = \frac{2\nu}{h}\,p'_{max}\,Gr_h^{1/2} \qquad \frac{\delta}{h} = q_\delta\sqrt{2}\,Gr_h^{-1/4} \qquad (72)$$

or

$$\frac{U\cdot\delta}{\nu} = 2\sqrt{2}\,p'_{max}\,q_\delta\,Gr_h^{1/4} \qquad \frac{U\cdot h}{\nu} = 2\,p'_{max}\,Gr_h^{1/2} \qquad (73)$$

and using the abbreviations $R_h = U\cdot h/\nu$ and $R_\delta = U\cdot\delta/\nu$ and substituting the numerical values for p'_{max} and q

$$R_\delta = 1.695\,Gr_h^{1/4} \qquad (74)$$

$$R_h = 0.550\,Gr_h^{1/2} \qquad (75)$$

Elimination of Gr_h from the last two equations gives the following expression as the relation between Re of the flow thickness and the height of the plate for a vertical plate in free flow:

---

[35]The distance from the lower edge is denoted by h instead of x, the nondimensional distance from the wall ξ by q, the nondimensional stream function ζ by p.

$$R_\delta = 2.29\ R_h^{1/2} \tag{76}$$

(b) Nusselt characteristics. - For the local heat-transfer coefficient $\alpha(h)$ at the height h above the lower edge, the following equation holds (ref. 21)*:

$$\alpha(h) = \lambda(-t_0')\ \frac{1}{h}\left(\frac{Gr_h}{4}\right)^{1/4} \tag{77}$$

($t_0' = -0.508$ is the value of the derivative of the nondimensional temperature function $t(q)$ for $q = 0$) or, in nondimensional form, the numerical values may be substituted:

$$\frac{\alpha(h)\cdot h}{\lambda} = 0.359\ Gr_h^{1/4} \tag{78}$$

The variation of the heat-transfer coefficient along the variable height h of a plate of total height H is most conveniently obtained by introducing a local heat-transfer coefficient which has been made nondimensional by dividing through by H

$$\frac{\alpha(h)H}{\lambda} = Nu_H(h) = 0.359\ Gr_H^{1/4}\left(\frac{h}{H}\right)^{-1/4} \tag{79}$$

The heat-transfer coefficient (fig. 18) at the lower edge of the plate with zero boundary-layer thickness is theoretically infinitely large and then continuously drops with the reciprocal of the fourth root of the height.

The mean heat-transfer coefficient corresponding to a plate of height H

$$\alpha_m = \frac{1}{H}\int_0^H \alpha(h)dh \tag{j}$$

is obtained from equation (77) as

$$\alpha_m = \frac{4}{3}\cdot\frac{\sqrt{2}}{2}\lambda(-t_0')\ \frac{1}{H}\ Gr_H^{1/4} \tag{80}$$

or, nondimensionalized and with numerical values substituted (fig. 18), as

$$\frac{\alpha_m H}{\lambda} = Nu_H = 0.479\ Gr_H^{1/4} \tag{81}$$

*Extrapolation.

4. Nondimensional Representation of Theory for Horizontal Cylinder

(a) Reynolds numbers. - The theoretical solution given previously for the tangential velocity u (eq. (55a)) and the distance n from the wall (eq. (55d)) for the azimuth x of a horizontal cylinder, with the values $n = \delta$ and the maximum velocity $u = U$, may be transformed to

$$U = \frac{\nu}{r} f(x)g(x)p'_{max} Gr_r^{1/2} \qquad \frac{\delta}{r} = \frac{q_\delta}{g(x)} Gr_r^{-1/4} \tag{82}$$

For the upper stagnation point $x = \pi$, because $g(\pi) = 0$ and $f(\pi) = 5.84$, the boundary-layer thickness becomes infinite and the tangential velocity zero. The quantity flowing through $U\delta$ and therefore the Re of the boundary layer $U\delta/\nu$, however, remain finite. To introduce Re for the characteristic length results in no simplication for the cylinder because, in addition to the characteristic length, the cylinder radius occurs as an additional characteristic length of the system. From equation (82),

$$U\delta/\nu = f(x)p'_{max} q_\delta Gr_r^{1/4} \tag{83}$$

Substituting the numerical values and using Gr_d result in the following expression for Re of the boundary layer at azimuth x:

$$R_\delta(x) = 0.357 f(x) Gr_d^{1/4} \tag{84}$$

and for Re of the boundary layer at the upper stagnation point (with $f(\pi) = 5.84$):

$$R_\delta = 2.08 Gr_d^{1/4} \tag{85}$$

where R_δ is written for $R_\delta(\pi)$. Although the theoretical solution for $x = \pi$ is no longer valid, equation (85) because of the small change of $f(x)$ gives the correct relations in the region of the upper stagnation point (up to about 165°), so that for the sake of simplicity the formula will be used in the following discussion.

(b) Nusselt characteristics. - Figure 18 shows the variation of the nondimensional local heat-transfer coefficient according to equation (60) over the developed semicircumference of the cylinder. In the region of the lower stagnation point, it has a finite, practically constant value; and at the upper stagnation point, it drops rapidly to zero in accordance with the upstreaming warm air at that point. In the same figure the mean heat-transfer coefficient Nu_d for a cylinder is plotted according to equation (65).

5. Hydrodynamic Comparison

(a) Between vertical plate and horizontal cylinder in free convection. - Although the boundary-layer growth for a vertical plate and a horizontal cylinder, as already remarked (Part III, sec. 1) and as seen from equations (72) and (82), differ fundamentally in character, it is nevertheless of interest to compare the flow condition (always characterized in what follows by R_δ) at the upper edge of the plate and in the region of the upper stagnation point of the cylinder. The following three questions will here be considered:

1. The behavior of the flow at the upper edge of the plate and at the upper stagnation point of the cylinder for the case that the height of the plate is equal to the cylinder diameter.

2. The behavior of the flow at the upper edge of the plate and at the upper stagnation point of the cylinder for the case that the height of the plate is equal to the developed semicircumference of the cylinder, that is, the characteristic lengths are equal.

3. The relation of the height of a plate whose flow condition at the upper edge is equal to that of the upper stagnation point of a cylinder to the diameter of the cylinder.

Before each of these questions is considered, the ratio of the boundary-layer Re numbers at the upper stagnation point of the cylinder $R_\delta(Z)$ and at the upper edge of the plate $R_\delta(P)$ are written, with the aid of equations (74) and (85):

$$R_\delta(Z)/R_\delta(P) = 1.226\ Gr_d^{1/4}/Gr_h^{1/4} \tag{86}$$

where $R_\delta(Z)$ and Gr_d refer to the cylinder, and $R_\delta(P)$ and Gr_h refer to the plate. The coefficient 1.226 has the following significance (cf. eqs. (85) and (83) for the cylinder, eqs. (74) and (73) for the plate):

$$1.226 = \frac{2.08}{1.695} = \frac{2^{-3/4} p'_{max} \cdot q_\delta \cdot f(\pi)}{2^{3/2} p'_{max} \cdot q_\delta} = \frac{f(\pi)}{4 \cdot 2^{1/4}} \tag{87}$$

1. For equal Gr of plate and cylinder, $Gr_d = Gr_h$, equation (86) gives

$$R_\delta(Z) = 1.226 \cdot R_\delta(P) \tag{88}$$

that is, for equal Gr of plate and cylinder, for example, for a plate of the height of the cylinder diameter $h = d$ under otherwise equal conditions (with regard to temperatures and materials), Re at the upper stagnation point of the cylinder is 22 percent greater than that of the upper edge of the plate (fig. 19). This result states nothing about the hydrodynamic relation between the two, since the comparison refers to different characteristic lengths. It is useful only for the rapid comparison of plate and cylinder for the usual values of Gr. It is then known that for equal Gr the cylinder possesses the more developed flow, so that the flow at the cylinder may be turbulent while that of the plate is still laminar.

2. For equal characteristic length $h = \pi/2d$ there is obtained from equation (86)

$$R_\delta(Z)/R_\delta(P) = 1.226\ (2/\pi)^{3/4} = 0.874 \qquad (89)$$

The boundary-layer Re at the upper stagnation point of a cylinder is thus 13 percent smaller than that of a plate of the height of the developed semicircumference of the cylinder (fig. 19). This retardation of the boundary-layer development as compared with the vertical plate is due to the fact that the boundary layer at the lower stagnation point of the cylinder already has a finite thickness, whereas in the case of the plate the thickness must increase from zero.

3. For equal boundary-layer Re values for the plate and cylinder, equation (86) gives

$$Gr_d/Gr_h = 1.226^{-4} = 0.441 \qquad (90)$$

At the upper stagnation point of the cylinder, there is therefore the same flow condition as at the upper edge of the plate if Gr of the cylinder is 0.44 times that of the plate. This permits a rapid conversion of the flow data for the plate into those for the cylinder and vice versa. If, for example, it is known from heat-transfer experiments on a plate that the departure from the laminar $Gr^{1/4}$ law occurs at $(Gr_h)_{kr} = 8\times10^8$, then it can be concluded without experiment from equation (90) that this must be the case for the horizontal cylinder for $(Gr_d)_{kr} = 3.5\times10^8$. If the plate and cylinder are under otherwise equal conditions, it is possible from equation (90) to derive a simple relation for the height of a plate h_a which is hydrodynamically equivalent to a cylinder:

$$d^3 : h_{\ddot{a}}^3 = 0.441 \qquad h_{\ddot{a}} : d = 1.311 \qquad (91)$$

In the neighborhood of the upper stagnation point of a horizontal cylinder, the same flow condition prevails (R_δ) as under otherwise equal conditions at a vertical plate of height 1.31 times that of the cylinder diameter (fig. 19). As was to be concluded from the answers to questions 1 and 2, this height must lie between the cylinder diameter and the developed semicircumference.

The answer to the three questions on the flow condition at a cylinder and at plates of various heights is shown in figure 19 (R_δ of the cylinder set equal to 1).

(b) Hydrodynamic comparison between a vertical plate in free convection and a plate in a parallel flow. - The relation (76) between Re of the boundary-layer thickness and that of the height of the plate (characteristic length) R_h for the vertical plate in free convection is strongly analogous to the corresponding relation (92) between Re of the boundary-layer thickness R_{δ^*} (referred to the displacement thickness δ^*) and the characteristic length R_x for a plate in a stream parallel to its plane (Blasius solution of the boundary-layer equations):

$$R_\delta = 2.29 \cdot R_h^{1/2} \quad (76) \qquad \| \qquad R_{\delta^*} = 1.73\, R_x^{1/2} \quad (92)$$

In spite of the already mentioned entirely different rate of growth of the boundary-layer thickness, in the case of the parallel flow as the square root of the distance from the incident edge and in the case of the free convection as the fourth root of distance from the lower edge, the development of the Reynolds number of the boundary-layer thickness as a function of the Reynolds number of the characteristic length in the case of these two very different types of flow follows the same exponential law and with approximately equal magnitude.

6. Thermal Comparison between Vertical Plate and Horizontal Cylinder

(a) Mean heat-transfer coefficients. - For equal Gr of plate and cylinder ($Gr_H = Gr_d$), there is obtained from equations (81) and (65) the following ratio of the nondimensional heat-transfer coefficients of the horizontal cylinder Nu_d and of the vertical plate Nu_H

$$Nu_d/Nu_H = 0.777 \quad (93)$$

Under otherwise equal conditions, therefore, the mean heat-transfer coefficient of a cylinder is only 78 percent of that of a plate of the

height of the cylinder diameter (fig. 18). In agreement with this, the comparison given by M. Jakob and W. Linke (ref. 19) of convection tests on vertical plates and horizontal cylinders in a single Nu-Gr diagram (with H and d denoting the length dimension) gives a lower position of the cylinder tests. The modified determination of the critical number, which follows from these results, will be discussed later (Part IV, sec. 5).

For equal mean heat-transfer coefficient α_m of plate and cylinder under otherwise equal conditions, there is obtained from equations (81) and (65)

$$0.479\ H^{-1/4} = 0.372\ d^{-1/4} \qquad H/d = 2.76 \tag{94}$$

The mean heat-transfer coefficient of a cylinder is therefore, under otherwise equal conditions, equal to that of a plate of height 2.76 times that of the cylinder diameter. On account of the small decrease of the local heat-transfer coefficient at large plate heights, this factor of 2.76 is not very sharply determined. Thus Jodlbauer (ref. 29) found it possible, without considering the previously given theoretical solution for the cylinder, to represent the mean heat-transfer coefficients for cylinders from tests by Koch by the formulas for the vertical plate if H is replaced by 2d (instead of theoretically by 2.76d). As a matter of fact, the α_m values thus determined for the cylinder lie only 8.3 percent above the values given by the theory according to equation (65), as can be seen by replacing H by 2d in equation (81).

(b) Total heat transfer. - The total heat transfer Q(Z) of a cylinder of diameter d along the entire circumference and the total heat transfer Q(P) along the two sides of a plate of the height H, under otherwise equal conditions, are in the ratio

$$\frac{Q(Z)}{Q(P)} = \frac{\alpha_m(Z)\pi d}{\alpha_m(P)2H} = \frac{\pi}{2}\frac{Nu_d(Z)}{Nu_H(P)}$$

and from equations (81) and (65),

$$Q(Z)/Q(P) = 1.221\ Gr_d^{1/4}/Gr_H^{1/4} \tag{95}$$

where the significance of the factor 1.221 is as follows (cf. eqs. (81), (80), (65), and (59)):

$$1.221 = \frac{\pi}{2}\frac{0.372}{0.479} = \frac{\pi}{2}\frac{2^{1/4}\bar{g}(-t_0')}{\frac{4}{3}\frac{\sqrt{2}}{2}(-t_0')} = \frac{3\pi\bar{g}}{4\cdot 2^{1/4}} \tag{96}$$

A comparison of this factor 1.221 with the factor 1.226 occurring in the ratio of the boundary-layer Re of cylinder and plate (eq. (86)) according to equation (87) shows that both are identical, since according to the theoretical solution, the following relation holds as an immediate consequence of the validity of the heat-transfer equation:

$$3\pi\bar{g} = f(\pi) \tag{97}$$

The small difference of 1/2 percent is explained by the fact that (as mentioned in connection with eq. (64)) $\bar{g}$ was computed not according to equation (97) but was obtained by planimetering.

For equal Gr_d and Gr_H values in equations (86) and (95), the following is thus obtained:

$$Q(Z)/Q(P) = R_\delta(Z)/R_\delta(P) \tag{98}$$

that is, the total heat transfer of a horizontal cylinder and that of the two sides of a vertical plate under otherwise equal conditions are in the same ratio as the boundary-layer Re values at the upper stagnation point of the cylinder and at the upper edge of the plate, respectively.

On the basis of relation (98) it is now possible, without further computation, to answer the three questions on the total heat transfer of a cylinder and plates of different height, analogous to the questions referring to the hydrodynamic comparison (see fig. 19; the heat transfer of the cylinder has been set equal to 1).

Corresponding to equation (88),

$$Q(Z) = 1.22\ Q(P) \tag{99}$$

The total heat transfer of a cylinder is thus 22 percent greater than that for the two sides of a plate of a height equal to the cylinder diameter under otherwise equal conditions (fig. 18).

Corresponding to equation (89),

$$Q(Z) = 0.87\ Q(P) \tag{100}$$

The total heat transfer of a cylinder is 13 percent smaller than that of the two sides of a plate of height equal to the developed semicircumference of the cylinder (equal characteristic length) under otherwise equal conditions.

Corresponding to equation (91) for

$$Q(Z) = Q(P)$$

there is obtained the height of a plate H_a' thermally equivalent to a cylinder:

$$H_a' : d = 1.31 \qquad (101)$$

The total heat transfer of a cylinder under otherwise equal conditions is therefore as great as for the two sides of a vertical plate of height 1.31 times that of the cylinder diameter. In summary it may therefore be stated that a horizontal cylinder and a vertical plate, which transfers heat on both its sides, of a height equal 1.31 times the cylinder diameter are equivalent both thermally (with reference to the total heat transfer) and hydrodynamically (with reference to the boundary-layer development at the upper stagnation point and at the upper edge, respectively).

IV. THE OCCURRENCE OF TURBULENCE IN FREE FLOW ABOUT A HORIZONTAL CYLINDER AND ALONG A VERTICAL PLATE

1. Introductory Observations

For the determination of the transition from laminar to turbulent flow in the case of free convection, tests were carried out on a vertical plate and a horizontal cylinder of sufficient size. Two main reasons underlay the investigation. In the first place, it was desired to determine the upper limit of the validity of the laminar boundary-layer theories for plate and cylinder and therefore the upper limit of applicability of the heat-transfer formulas developed from these theories for practical application. The second reason was of a more theoretical nature. The numerous turbulence investigations, both experimental and theoretical, undertaken in recent decades have been concerned almost exclusively either with the flow between two parallel walls with linear velocity distribution (Couette flow) or with the flow in pipes, channels, about rotating cylinders, along plates, cylinders, or other resistance bodies which have in common a velocity profile which rises uniformly from the value zero at the wall up to a maximum value. Differing essentially from these profiles are evidently velocity profiles for which the velocity rises from the value zero at the wall to a maximum value and then, after passing through a point of inflection, again drops to the value zero at a large distance from the wall. Such profiles are typical in the case of heat transfer by free convection.

Some further observations on the setting up of turbulence in free convection will be made later in connection with the discussion of results (sec. 5).

2. Test Procedure

For the investigation, the schlieren method developed by E. Schmidt was applied, which as an optical method provides the possibility of an instantaneous view of the entire field, and is therefore of advantage for determining the critical number.

The schlieren method has been described in detail by E. Schmidt (ref. 22) so that only the essential points will be given here. It is based on the deflection suffered by a light ray in passing through a field with density stratification (i.e., variation of the index of refraction) normal to its direction of propagation toward the colder layer. In the test, a parallel light beam is allowed to pass tangentially along the surface of the heated body. The rays in the neighborhood of the wall, because of the maximum temperature drop at that place, are most strongly deflected from their initial direction; those farther away from the wall are less deflected, while those rays which are outside the temperature field undergo no deflection. On a screen which is set up at a sufficient distance behind the heated body, the rays near the wall appear the farthest from the wall. The following picture is obtained: the heated body throws a completely dark shadow which, as compared with that of the cold body, is increased by the thickness of the temperature boundary layer. This shadow is bounded by a first "interior caustic curve" adjacent to which is formed a medium-bright region (rays which have passed through the temperature field), which in turn is bounded toward the outside by a second "external caustic curve" originating from the tangential rays in the neighborhood of the heated surface. Still farther toward the outside is the uniformly bright field of the undisturbed illumination.

For an accurate evaluation, the method is suitable only for bodies having one of its length dimensions (two-dimensional problem), so that the effect of the temperature fields at the ends on the path of the light ray is small compared with the deflection undergone in passing through the distance along the length. On the other hand, the length should be chosen only large enough so that the light ray at the end of the body still is approximately at the same distance from the wall as at the initial point of the body.

3. Test Setup and Procedure[36]

(a) Plate. - The plate was 100 by 100 centimeters and 1.0 centimeter thick. It consisted of two zinc sheet plates 1 millimeter thick which by interposing a frame of 8-millimeter U-brass were soldered onto each other. In the interspace there was placed a heating coil, insulated by asbestos boards, which consisted of 36 meters of chrome-nickel wire of 1-millimeter diameter with a total resistance of 51 ohms. In air of room temperature, the plate could be kept at 100° C surface temperature with 5.6 amperes. The plate was suspended on two bicycle wheel spokes which were attached to the upper strip of the frame. Through the latter the current was also conducted to the interior. For measuring the surface temperature a silver-constantan thermocouple was used which was flatly soldered on about 5 centimeters from the upper rim of the plate and the wires of which extended a few more centimeters quite close to the plate. This simple temperature measurement could be applied because extreme accuracy was not required. Figure 20 shows the plate suspended with the current-supplying wires, and the thermocouple and two pendulums each with two spheres which served to determine the vertical and made possible the mutual comparison of the different photographs.

(b) Cylinder. - The cylinder consisted of two layers of 0.7-millimeter-thick zinc sheet which was rolled over two bicycle wheel rims and soldered to their upper sheathing strip. Between the sheets there was placed the heating coil insulated by asbestos board, the coil being of 54 meters of chrome-nickel wire of 1-millimeter diameter with a total resistance of 77 ohms, which brought the cylinder in air of room temperature to 100° C surface temperature with a current of 4.1 amperes. The cylinder was suspended on two bicycle wheel spokes. The current leads and thermocouple were similarly located on the upper sheathing strip. The mean length of the cylinder was 100.2 centimeters, and its mean outer diameter 58.45 centimeters (fluctuating between 58.35 in the horizontal and 58.75 over the soldered seam). The frontal surfaces were closed off with asbestos board. Figure 21 shows a view with the suspension, current leads, and the two pendulums.

(c) Setup. - Since it is very difficult to produce a parallel bundle of rays of the diameter of the body here employed by means of lenses, such a beam was replaced by the light from a strongly screened (as a rule of 3-mm aperture) arc lamp 32 meters from the heated body. The distance between the body and the screen was 8 meters. The apparatus was set up on the largest floor, of 42-meter length, of the

[36]Acknowledgment is made to Herr Dr. R. Weise and Dr. H. Kurzweg, Leipzig. For the test setup, acknowledgment is made to Master Mechanic G. Hentsch, Leipzig.

Institute. Because of the window in one of the walls and the connection to the staircase halls, it was not possible to exclude entirely currents of the room air so that only at high temperature differences (above 50° C) could useful schlieren photographs be obtained. The existing dissymmetry of the critical points on the two sides of the bodies, both for the plate and cylinder (see table V) was due to a unilateral convection flow from the window wall. The horizontal adjustment of the test bodies was effected by means of a water balance; the adjustment parallel to the light cone, by measuring the shadow of the cold body.

(d) Photography[37]. - The schlieren pictures were obtained by two methods. In one method the shadow pictures were taken on the screen by means of a lens and camera (13×18 cm, Zeiss-Tessar 1:2.7). In spite of highly sensitive plates (Agfa-Superpan 16/10 DIN), exposure times of 5 to 25 seconds were required on account of the low brightness, because of the strong screening and large distance from the arc lamp. For determining a time mean value of the fluctuating critical points, these time pictures were, however, particularly well suited. The photograph was taken either somewhat from the side (plate) or, in order to avoid distortions, exactly central (partly in the case of the cylinder); the camera was set up in the shadow of the cylinder so that the legs of the tripod threw an additional shadow (fig. 23). The second method consisted of a direct illumination of one or several photoplates simultaneously (Agfa-Isochron 13/10 DIN, 10×15 cm), which were brought to the position of the screen. The greater brightness obtained in this way made possible instantaneous photographs (through light flashes from the arc lamp), which in connection with their greater scale provided a view in instantaneous detail of the transition from laminar to turbulent flow.

4. Evaluation of the Schlieren Pictures

Figures 22 and 23 show time exposures of the plate and cylinder taken by means of lens and camera. In the center the magnified shadow of the body by the thickness of the temperature boundary layer, the "inner caustic curve" surrounding it, and further toward the outside the "outer caustic curve" arising from the rays near the wall. The dissymmetry of the lower edge of the plate is due to the disturbances of the room air that were mentioned previously. The upper edge of the plate is immediately below the frame of the picture in the "necking" of the central shadow. In the upper stagnation point of the cylinder are seen the shadows of the suspension wires, current leads, and thermocouple wires; below are seen the three tripod legs for the central

[37]For valuable advice in connection with the photography, acknowledgment is made to Herr Dr. A. Naumann, Leipzig.

photograph. Figure 24 shows for simultaneously obtained instantaneous photographs of the left[38] side of the plate (in the case of direct illumination about 25 cm from the lower edge starting with small interspaces of about 1 cm), a region of about 50-centimeter height: at 24(a) and the lower part of 24(b), laminar; in the upper part of, 25(b), a transition; 24(c) and 24(d), turbulent. Figure 25 shows three simultaneously taken instantaneous pictures of the cylinder with direct illumination: 25(a) at the lower stagnation point, laminar; 25(b) at the left azimuth of 120°, turbulent; 25(c) at the upper stagnation point, warm air stream.

As shown by figures 22 to 25, the outer caustic curve of the rays near the wall is particularly suitable for determining the critical location. If this line is broken up, then turbulence certainly exists; whereas the flow regions farther from the wall are more easily disrupted through external disturbances. In the laminar (lower) region, the caustic curve is sharp and is completely stationary; in the turbulent (upper) region it is torn into several pieces and in disordered motion. In the time photographs, this means complete washing out. The critical position itself fluctuates upwards and downwards, at one time very rapidly and at another slowly. For evaluating the time photographs there was taken as the "time mean value of the critical position" the end of the region in which the existence of an outer caustic curve through differences in brightness could still be determined outwards and inwards (arrows). Above the critical position the heated layer rises as a whole outwards as broad, uniformly bright strips. Comparison of the photographic observation thus determined with the mean critical position estimated from naked eye observation over a period of time showed good agreement and therefore the justification of this procedure.

The critical positions obtained by this procedure are collected together with the remaining test values in table V. Each critical point is the mean value of four determinations two of which were made with direct illumination, and two with a magnified projection picture. The Gr values are formed in the case of the cylinder with the diameter, in the case of the plate with the critical height as characteristic length. By means of equation (74) for the plate and, with $f(x_{kr})$, equation (84) for the cylinder, the critical Reynolds numbers of the boundary appearing in the last column were computed. Their mean values of 303 for the plate and 285 for the cylinder are weighted according to the different illimination times of the individual pictures. From the mean value $R\delta_{kr} = 303$ the value 1.0×10^9 is obtained for the mean critical Gr for the plate.

[38] On the right of the figure; the pictures with direct illumination are laterally interchanged.

5. Discussion of Results

The mean value of 303 for the critical Reynolds number of the boundary later for the plate and 285 for the cylinder can be regarded in agreement, in view of the accuracy of determination of a critical number in general and the small number of the schlieren pictures and disturbances of the room air in particular. This is understandable from the fact that the velocity profiles of both flow processes at any distance from the lower edge or lower stagnation point are affine to each other. The development along the initial stretch occurs in a different manner, but this should have only a higher-order effect. As was to be expected, the critical number of the free profile $R_{\delta_{kr}} \approx 300$ lies considerably below the critical number of the profile in the case of forced flow (plate), which, referred to the displacement thickness of Burgers and Hansen, amounts to 950 in the wind tunnel, and according to more recent tests in the Göttingen water tunnel for very quiet approach, it amounts to about 1400. It would be of interest to know whether a theoretical stability investigation for the free profile, the analog of the familiar computations in the forced-flow case, would have to be conducted in order to give this increased instability.

With the determination of the critical number for the vertical plate and the horizontal cylinder and reduction to the critical Reynolds number of the boundary layer, the data of other investigators will be compared with regard to the transition from laminar to turbulent flow.

E. Schmidt (ref. 26) notes that according to tests in air, the flow at about 100° C plate temperature remains laminar up to a plate depth of about 50 centimeters, corresponding to a critical Gr of 8×10^8, in good agreement with the values obtained herein.

M. Jakob and W. Linke (ref. 19) determined from a combination of the measurements of various investigators on vertical plates, vertical and horizontal cylinders, block, and sphere, as the transition point from the $Gr^{1/4}$ to the $Gr^{1/3}$ law, the critical number of $(Gr \cdot Pr)_{kr}$ 3.0×10^7, that is, for diatomic gases $Gr_{kr} \approx 4.0\times10^7$. The difference as compared with the present determinations should in large part be ascribed to the fact that hydrodynamically unequivalent bodies (Reynolds number of the boundary, see Part III, sec. 5a, eq. (88)) were here treated together. If account is taken only of the tests on the vertical plates and vertical cylinders (Part III, sec. 6a), which for large cylinder diameters and large Gr (thin boundary layer) are at least approximately equivalent hydrodynamically, there is obtained a critical Gr of 4×10^8, which is therefore quite close to the present determinations.

E. Griffith and A. H. Davis (ref. 17) investigated the local distribution of the heat transfer on a 270-centimeter-high wall, which consisted of 25 individual elements. They obtained a minimum value of the heat transfer at about 38-centimeter height (their own determination) which they regarded as the transition from the laminar to the turbulent condition. This agrees in order of magnitude with the present values (columns between the individual elements), where it should be further clarified which point of their curve is to be regarded as the "critical point" proper.

6. Travel of the Critical Azimuth for the Horizontal Cylinder

On the basis of the given theoretical solution of the flow about the horizontal cylinder and the point of transition experimentally determined for a $Gr \approx 10^9$, the travel of the critical azimuth for a variable Gr can be computed if it is assumed that the turbulence always occurs if the boundary-layer Re has the same value of 285. This reasonable assumption will correspond all the more to fact since, as has just been shown, even for the vertical plate with a quite different boundary-layer development, the turbulence is set up at the same critical number of the boundary layer.

From equation (84), the following relation is obtained, with the value $R_{\delta_{kr}} = 285$:

$$(Gr_d)_{kr} = \left(\frac{800}{f(x_{kr})}\right)^4 \tag{102}$$

which is evaluated in table VI and plotted on semilogarithmic grid in figure 26. In accordance with the basic considerations, for a $Gr = 10^9$ the start of turbulence occurs for an azimuth of about 120°. Completely laminar flow about the cylinder, for extension of the theory up to the upper stagnation point, occurs for $Gr < 3 \times 10^8$. The transition point reaches the equator for $Gr = 3 \times 10^9$.

For greater clarity, the Gr will be expressed for cylinders of varying diameters, which are in air of 20° C with a surface temperature of 100° C. From the definition of Gr, for $\theta = 80$ (°C), $\beta = 1/293$ ($^\circ C^{-1}$), $\nu(100^\circ) = 0.231$ (cm^2/sec), the following relation obtains:

$$d\,[cm] = \left(\frac{Gr_d}{5.01} \times 10^3\right) 1/3 \tag{103}$$

which with the aid of the critical Gr_d values from equation (102) has similarly been evaluated in table VI and plotted in figure 27. Corresponding to the basic considerations, the critical azimuth for the

relations considered for a cylinder of 60-centimeter diameter is 120°. For cylinders below 41 centimeters, no turbulence occurs at all. The transition point reaches the equator for a cylinder of 84-centimeter diameter.

For practical applications, the result is thus obtained that for heated horizontal conducting pipes up to 40 centimeters in diameter and surface temperatures of 100° C in room-temperature air the previously given formulas are valid for the heat transfer in air (in particular, eqs. (60) and (65)). For accurate computation, the nondimensional formulation of figure 26 is naturally to be applied. The formulas can, in the absence of other suitable data, still be applied up diameters of 60 centimeters, because two thirds of the cylinder periphery is still in laminar flow. There should not likewise be much of a change for considerably higher surface temperatures (200° or 300° C).

The experimental determination of the variation of the critical azimuth for the cylinder with the Gr, through varying the temperature, remained unsuccessful. For temperature difference up to about 50° C the outer caustic curve is still not sufficiently far from the central shadow in order to be perceived separately from the latter, as is required for determining the critical number. For this, the distance between the cylinder and the screen would have to be considerably increased, which is not possible on account of space requirements. Going beyond the usually employed temperature differences of 80° C, because of the strong increase in ν, no longer gives an increase in Gr and moreover gives increasingly stronger deviations from the assumption of moderate temperature differences, which is at the basis of the theory. The travel of the critical azimuth with Gr is best determined by varying the cylinder diameter, as follows from figure 27.

V. SUMMARY

From the numerous tests already available on the heat transfer from horizontal pipes and wires in diatomic gases, the dependence of the nondimensional heat-transfer number Nu on the Grashof number Gr and the temperature coefficient Te, which enters as a further nondimensional factor at large temperature differences, is determined. The effect of Te on the heat transfer is quantitatively determined for the first time. It is particularly large in the region of small Gr (10^{-4} to 10), where on the average a decrease in Nu by 22 percent for increase of Te from Te = 0 to Te = 1 is obtained. The experimentally found dependence of Nu on Gr, Pr, and Te can then obtain a qualitative theoretical explanation.

For the region of Gr (about 10^4 to 3×10^8) in which the heat transfer is limited to a thin (in comparison with the cylinder diameter), heated layer with laminar flow, the velocity and temperature fields and the heat transfer are quantitatively computed from the boundary-layer differential equations without any additional empirical values; these computations are found in good agreement with the available measurements. In particular, the one-fourth power law of the heat transfer is obtained theoretically as $Nu = 0.37\ Gr^{1/4}$.

The flow and heat-transfer relations thus computed (Re of the boundary-layer flow, variation of the local heat-transfer coefficient along the cylinder periphery, mean heat-transfer coefficient, and total heat given off by the cylinder) are compared with the already known relations for the vertical plate. Among other results, the depth of a vertical plate is determined which for free convection shows equal flow condition and equal total heat transfer at a given cylinder, so that a simple computation is made possible for converting the heat-transfer data for a plate to those of a cylinder and conversely.

In order to know the upper limit of validity of the laminar-flow and heat-transfer computations and the laminar heat-transfer formulas, the start of turbulence was determined by schlieren photographs on a vertical plate and a horizontal cylinder of sufficient size. This occurs for different values of Gr, namely, $Gr = 1.0\times10^9$ for the plate and $Gr = 3.5\times10^8$ for the cylinder, but for equal Re of the boundary-layer flow, namely, for $Re \approx 300$. In this way, the critical Reynolds number of the velocity profile of the free flow was determined for the first time; as compared with other velocity profiles, this profile is marked by the presence of a maximum value and a point of inflection. Likewise computed with the Grashof number was the 'critical azimuth' on the cylinder at which the laminar flow passes into the turbulent flow.

REFERENCES

1. Hermann, E.: Phys. Z., Bd. 33, 1932, p. 425.

2. Nusselt, W.: Gesundh. Ing., Bd. 38, 1915, p. 477.

3. Davis, A. H.: Coll. Res. Nat. Phys. Lab., vol. 19, 1926, p. 193. (See also Phil. Mag., vol. 43, 1922, p. 329.)

4. Gröber, H., und Erk, S.: Die Grundgesetze der Wärmeübertragung. Julius Springer Berlin, 1933.

5. Schmidt, H.: Ergebn. exakt. Naturwiss., Bd. 7, 1928, p. 342.

6. Gröber, H.: Wärmeübertragung, Julius Springer (Berlin), 1926.

7. Ayrton, W. E., and Kilgour, H.: Phil. Trans. Roy. Soc. (London), vol. A183, 1892, p. 371.

8. Langmuir, I.: Phys. Rev., vol. 34, 1912, p. 401.

9. Langmuir, I.: Trans. Am. Inst. Elec. Eng., vol. 31, 1912, p. 1229. (See also Proc. Am. Inst. Elec. Eng., vol. 32, 1913, p. 407.)

10. v. Bijlevelt, J. S.: Die künstliche Konvektion an elektrischen Hitzdrahte. Diss., T. H. Dresden, 1915.

11. Kennelly, A. E., Wright, C. A., and v. Bijlevelt, J. S.: Trans. Am. Inst. Elec. Eng., vol. 28, 1909, p. 363.

12. Petavel, J. E.: Phil. Trans., Bd. (A)197, 1901, p. 229.

13. Wamsler, F.: VDI Forschungsheft 98/99 (Berlin), 1911.

14. Nusselt, W.: Diss. T. H. München, 1907.

15. Koch, W.: Beih. z. Gesundh.-Ing. Reihe 1, Heft 22 (Berlin und München), Oldenbourg 1927.

16. Jodlbauer, K.: Forsch. Ing.-Wes., Bd. 4, 1933, p. 157.

17. Griffiths, E., and Davis, A. H.: Transmission of heat by radiation and convection. (London), 1931.

18. King, W. J.: Mech. Eng., vol. 54, 1932, p. 347.

19. Jakob, M., and Linke, W.: Forsch. Ing.-Wes., Bd. 4, 1933, p. 75.

20. Davis, A. H.: Phil. Mag., vol. 44, 1922, p. 920.

21. Schmidt, Ernst, und Beckmann, Wilhelm: Das Temperatur- und Geschwindigkeitfeld vor einer Wärme abgebenden senkrechter Platte bei natürlicher Konvektion. Tech. Mech. u. Thermodynamik, Bd. 1, Nr. 10, Okt. 1930, pp. 341-349; cont., Bd. 1, Nr. 11, Nov. 1930, pp. 391-406.

22. Schmidt, E.: Forsch. Ing.-Wes., Bd. 3, 1932, p. 181.

23. Hermann, R.: Phys. Z., Bd. 34, 1933, p. 211.

24. Beckmann, W.: Forsch. Ing.-Wes., Bd. 2, 1931, p. 165.

25. Weise, R.: Forsch. Ing.-Wes., Bd. 6, 1935, p. 281.

26. Jakob, M., und Linke, W.: Phys. Z., Bd. 36, 1935, p. 275.

27. Schmidt, E.: Z. VDI, Bd. 76, 1932, p. 1025.

Translated by S. Reiss
National Advisory Committee
for Aeronautics

TABLE I. - SUMMARY OF TESTS BY DIFFERENT INVESTIGATORS

Investigator	Ayrton, Kilgour	Langmuir	Bijlevelt	Kennelly, Wright, Bylevelt	Petavel	Wamsler	Koch
Substance	9 Pt wires	5 Pt wires	6 wires: Ta, Pt, Fe, Cu, Ag, Ni	3 Cu wires	1 Pt wire	Pipes: 6 wrought Fe; 6 Cu; 1 cast Fe	4 steel pipes
Cylinder diam., cm	0.0031-0.0356	0.00404-0.0510	0.0043-0.1000	0.01143-0.06907	0.1106	2.05-8.9 5.9 5.9	1.4-10.05
Temperature of body, t_w, °C	40-300	227-1027	46-239	-------	------	---	27.6-188.6
Excess temperature, θ, °C	------	--------	------	15-180	200-1000	36-243	13-174.4
Room temperature, t_∞, °C	10.5-15.9	27	17-22	20 (approx)	16	10-29	14.2-22
Medium	Air	Air	Air	Air	Air, H_2, O_2	Air	Air
Pressure, mm Hg	750	750	750	120-1900	0.12-160 atm	715	715.7-722.3
Cylinder length, cm	32.5	100	35	150 (approx)	45	300	138-198
Surrounding space	Horizontal pipe: length, 32.5 cm; diam. 5.08 cm	Base, 100× 15 cm^2; height, 30 cm	Height, 300 cm	Vertical tank: length, 152 cm; height, 660 cm	Horizontal pipe: length, 45 cm; diam. 2.06 cm	Base, 7.35 sq meters; height, 210 cm	Height, 400 cm
Ratio of space height to cylinder diam.	1640:143	7430:588	70,000:3000	58,200:9640	18.6	102:24	286:40
Te number	0.30-1.00	0.67-3.33	0.097-0.758	0.052-0.61	0.69-3.46	0.13-0.82	0.045-0.606
Relative decrease of Nu for $\Delta Te = 1$, percent	7.6-16.8	7.2-2.2	8.4-45.6	25.2	Irregular	None	None
Mean value of Nu for $\Delta Te = 1$, percent	13.2	Systematic	25.6	25.2	---------	----	----
Figure	1	2	3	4	5	6	7

TABLE II. - VALUES FOR THE MOST PROBABLE HEAT-TRANSFER LAW IN DIATOMIC GASES

[Nu as function of Gr with Te as parameter for Pr = 0.74.]

	log Gr Gr	-4 10^{-4}	-3 10^{-3}	-2 10^{-2}	-1 10^{-1}	0 1	1 10^{1}	2 10^{2}	3 10^{3}	4 10^{4}	5 10^{5}	6 10^{6}	7 10^{7}	8 10^{8}
Te=0	log Nu Nu	0.685-1 .484	0.716-1 .520	0.787-1 .612	0.908-1 .809	0.040 1.10	0.176 1.50	0.321 2.18	0.476 2.99	0.650 4.47	0.850 7.08	1.094 12.4	1.344 22.1	1.594 39.3
Te= 0.65	log Nu Nu	0.618-1 .415	0.649-1 .446	0.719-1 .524	0.838-1 .688	0.985-1 .966	0.134 1.86	0.290 1.95	0.458 2.87	0.645 4.42	Same as for Te = 0			

TABLE III. - NORMED AZIMUTH FUNCTIONS F(x) AND G(x) AS SOLUTION OF DIFFERENTIAL EQUATION SYSTEM (28) WITH BOUNDARY CONDITIONS ACCORDING TO EQUATION (29)

[F^{I} solution of eq. (33I); F^{II} solutions of eq. (33II).]

x	0^{o}	30^{o}	60^{o}	90^{o}	120^{o}	150^{o}	165^{o}	180^{o}
F'	0.0007	0.518	1.025	1.504	1.936	2.298	2.433	2.560
F"	(-0.23)	.456	1.018	1.504	1.941	2.352	(2.55)	2.763
G	1.000	.989	.945	.873	.765	.602	.473	0

TABLE IV. - FINAL AZIMUTH FUNCTIONS f(x) AND g(x) AS SOLUTION OF DIFFERENTIAL EQUATION SYSTEM (24) WITH BOUNDARY CONDITIONS OF EQUATIONS (26a) TO (26c)

x	0°	30°	60°	90°	120°	150°	165°	180°
f	0	1.181	2.337	3.430	4.41	5.24	5.55	5.84
g	0.760	.752	.718	.664	.581	.458	.360	0
f·g	0	.887	1.678	2.274	2.565	2.397	1.995	0

TABLE V. - EVALUATION OF SCHLIEREN PHOTOGRAPHS FOR OCCURRENCE OF TURBULENCE

(a) Vertical plate.

Number	b, mm	t_∞, °C	Exposure time, sec	t_w, °C	Critical height, h_{kr}, cm			Gr_{hkr}	$R_{\delta kr}$
					Left	Right	Middle		
24	748	16.5	20	78	76.0	55.9	66.0	13.42×10^8	324
25	748	16.5	20	113	53.8	47.3	50.6	6.83×10^8	274
26	748	16.5	25	100	66.2	60.8	63.5	13.13×10^8	323
27	748	16.5	20	100	60.9	47.3	54.1	8.12×10^8	286

Mean: 303

(b) Horizontal cylinder. Diameter, d, 58.45 centimeters.

Number	b, mm	t_∞, °C	Exposure time, sec	t_w, °C	Critical azimuth, x_{kr}			Gr_{hkr}	$f(x_{kr})$	$R_{\delta kr}$
					Left	Right	Middle			
6	760	19	10	102	125.5°	123.5°	124.5°	10.26×10^8	4.55	291
10	760	19	20	102	125.8°	110.0°	117.9°	10.26×10^8	4.35	278
11	760	19	5	102	120.9°	116.0°	118.5°	10.26×10^8	4.37	279
12	760	19	20	102	126.7°	117.6°	122.1°	10.26×10^8	4.48	286
17	752	18	20	102	123.8°	115.0°	119.4°	10.23×10^8	4.39	281
18	752	18	5	102	144.5°	129.5°	137.0°	10.23×10^8	4.90	313

Mean: 285

TABLE VI. - TRAVEL OF TURBULENCE TRANSITION POINT (CRITICAL AZIMUTH x_{kr}) WITH GRASHOF NUMBER OF CYLINDER Gr_d OR WITH CYLINDER DIAMETER d

[t_w, 100° C; t_∞, 20° C; b, 760 mm.]

x_{kr}	180°	165°	150°	120°	90°	60°	30°	15°	10°	5°
Gr_d	3.52×10^8	4.30×10^8	5.42×10^8	1.07×10^9	2.96×10^9	1.37×10^{10}	2.10×10^{11}	3.35×10^{12}	1.69×10^{13}	2.72×10^{14}
d, cm	41.3	44.1	47.7	59.9	84.0	140	347	890	1500	3790

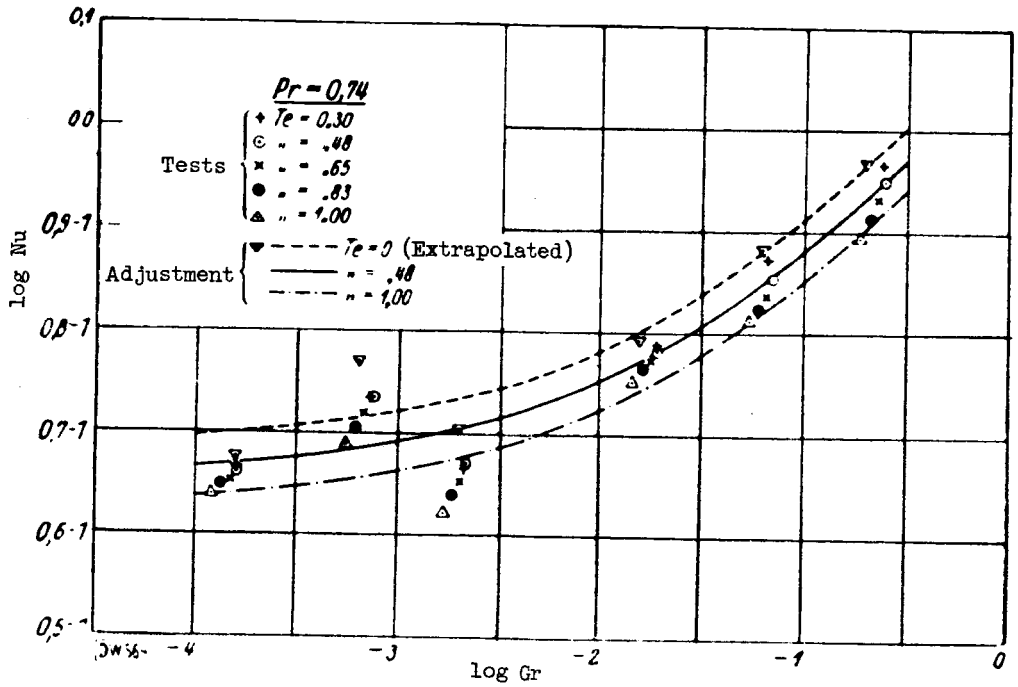

Figure 1. - Convection tests of Ayrton and Kilgour on nine platinum wires.

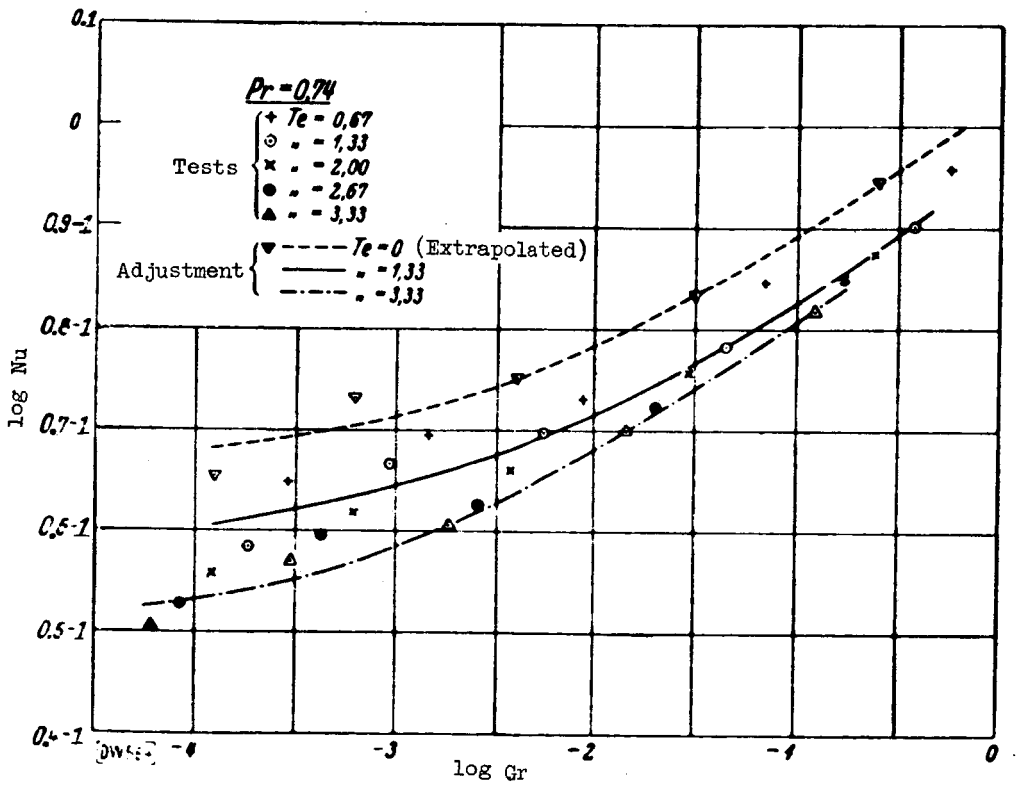

Figure 2. - Convection tests of Langmuir on five platinum wires.

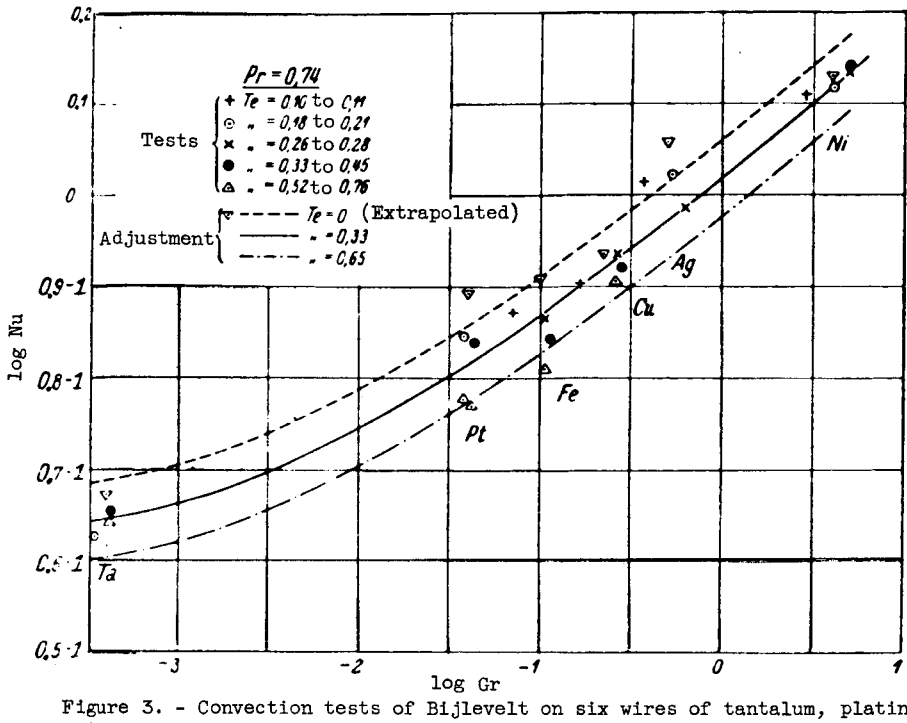

Figure 3. - Convection tests of Bijlevelt on six wires of tantalum, platinum iron, copper, silver, and nickel.

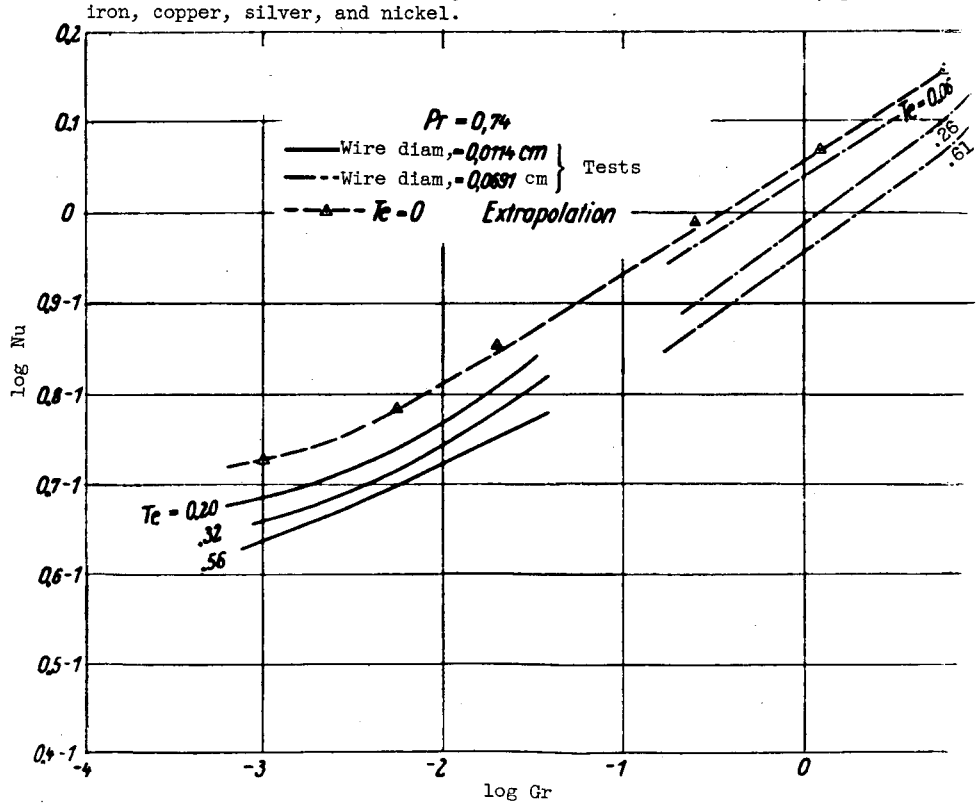

Figure 4. - Convection tests of Kennelly, Wright, and Bijlevelt on three copper wires.

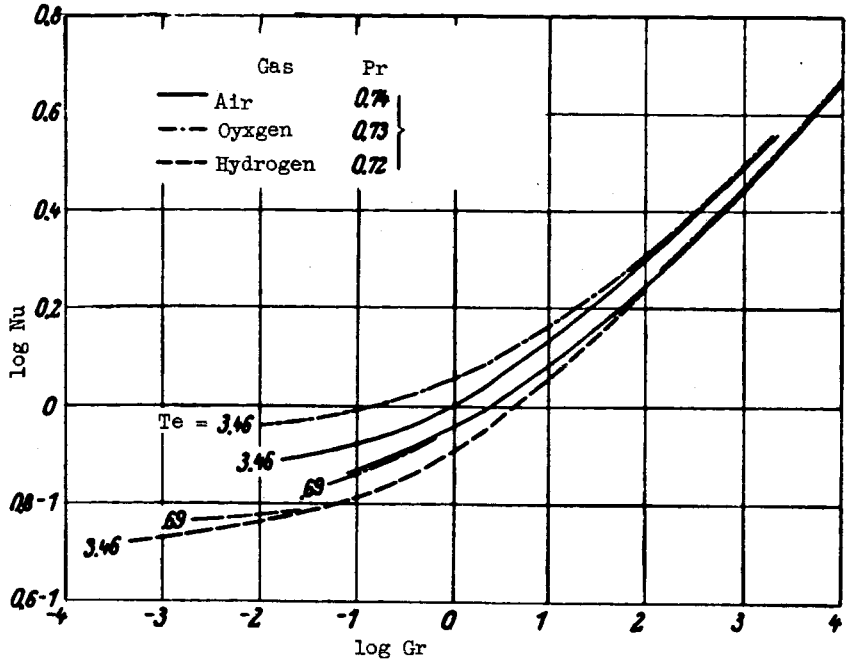

Figure 5. - Convection tests of Petavel on one platinum wire.

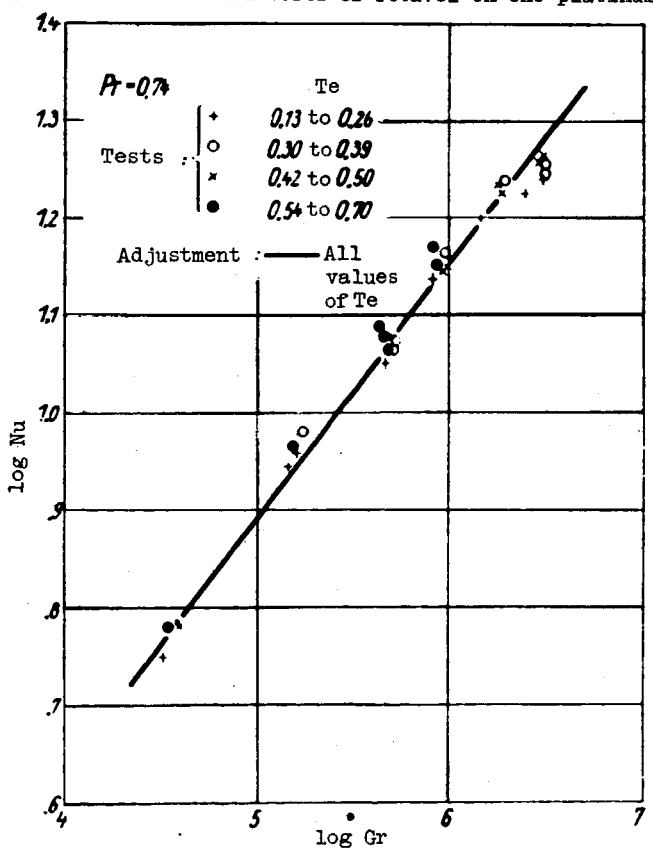

Figure 6. - Convection tests of Wamsler on one copper, one cast iron, and six wrought iron pipes.

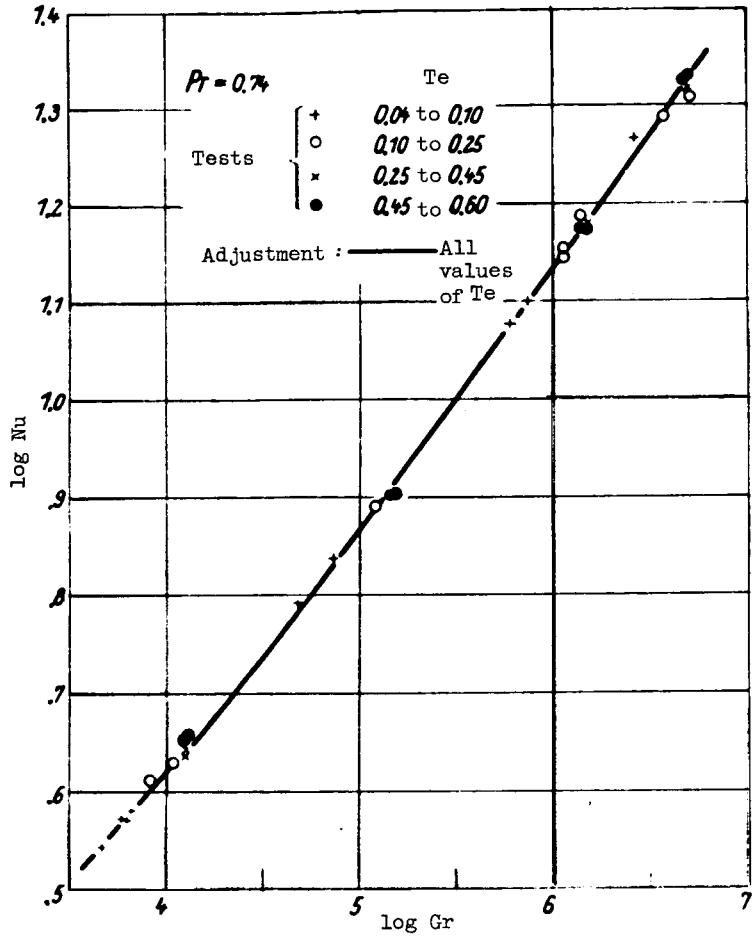

Figure 7. - Convection tests of Koch on four steel pipes.

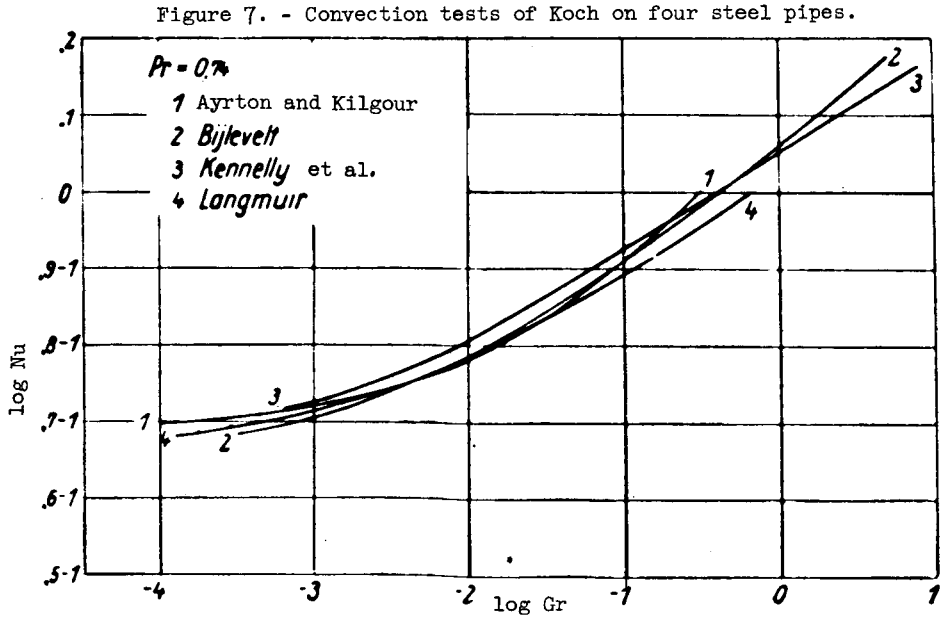

Figure 8. - Comparison of test results of different investigators for Te = 0 (extrapolated). Limiting law of small temperature differences.

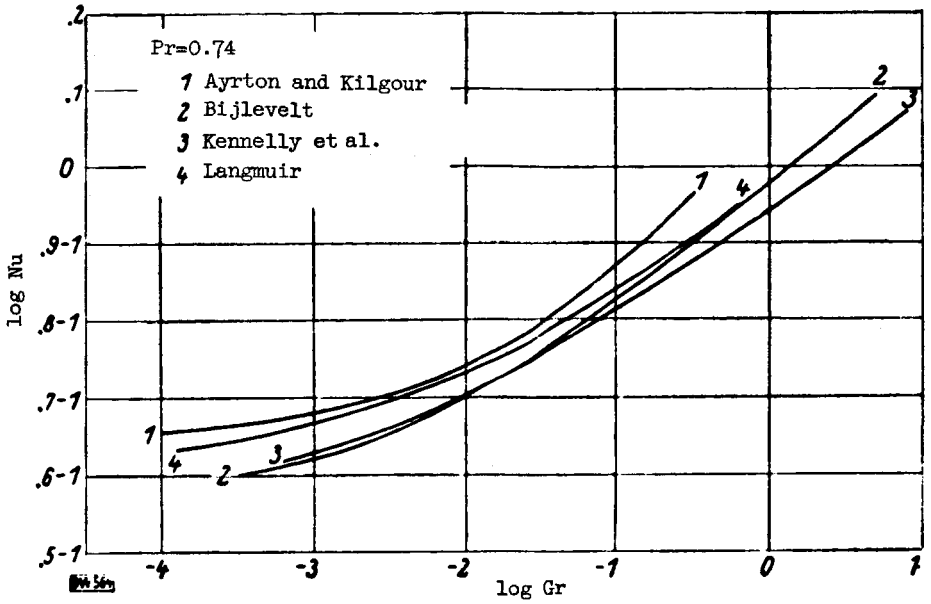

Figure 9. - Comparison of test results of various investigators for Te = 0.65.

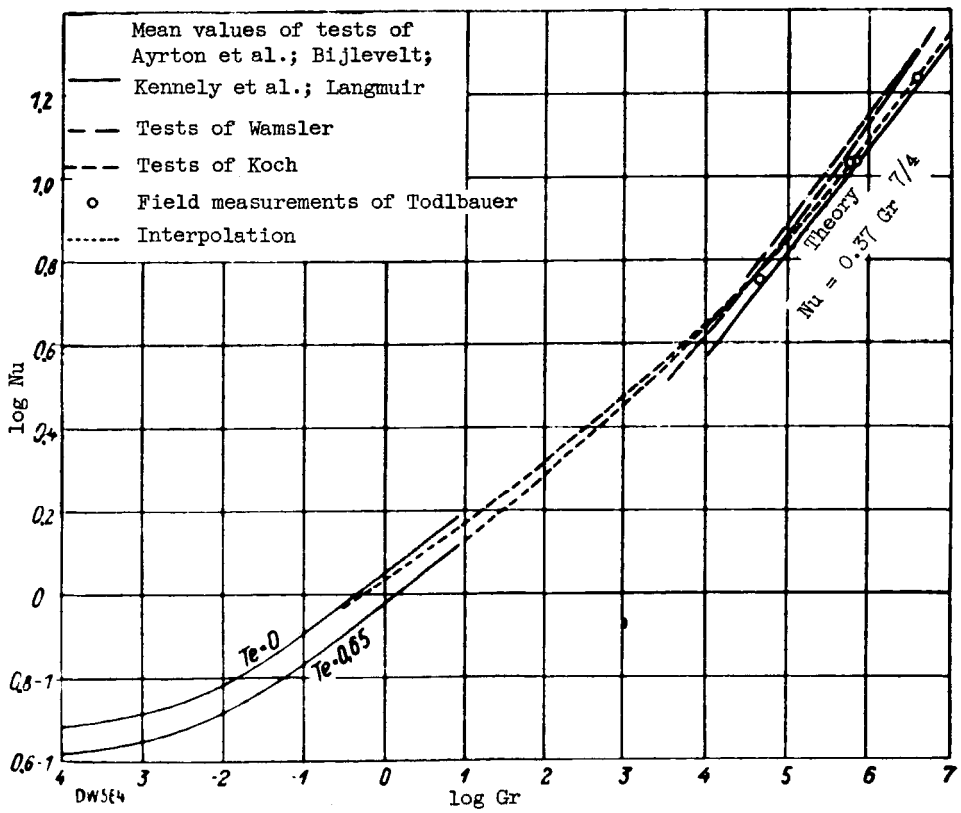

Figure 10. - Summary of all test results with diatomic gases (Pr = 0.74) with the adjustment curve giving the most probable heat-transfer law based on present information.

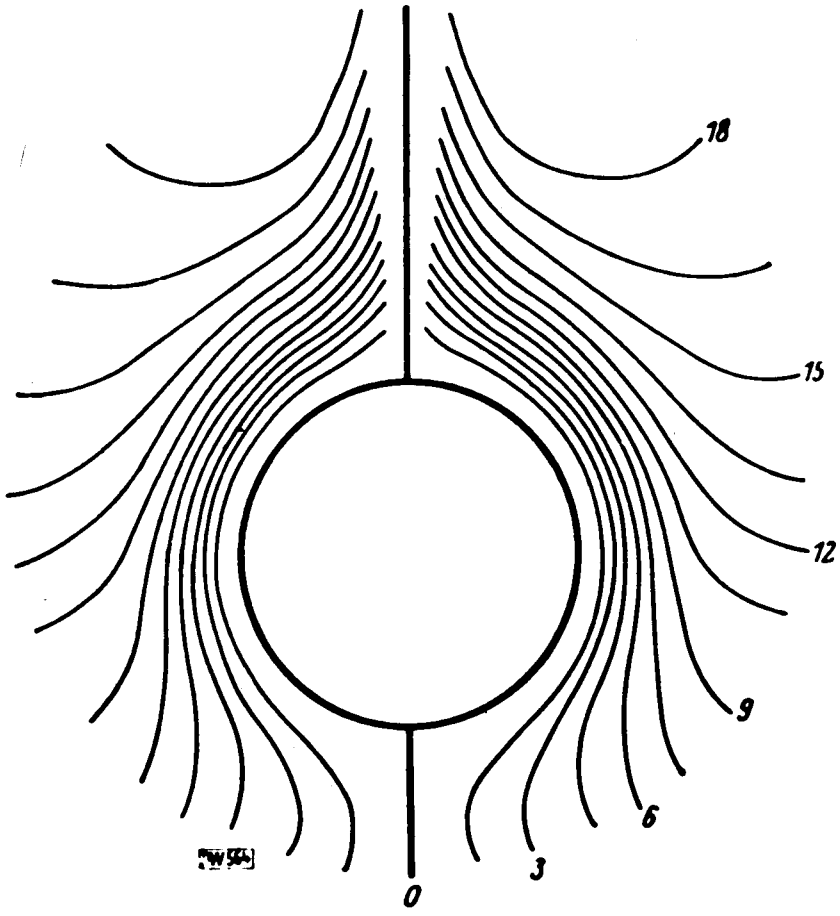

Figure 11. - Theoretical streamlines for horizontal cylinder. The numbers give the values for ψ/ν. Scale is for Gr = 10^4: For Gr = 10^6, the distances from the surface are to be shortened by 1/3.16; for Gr = 10^8, by 1/10.

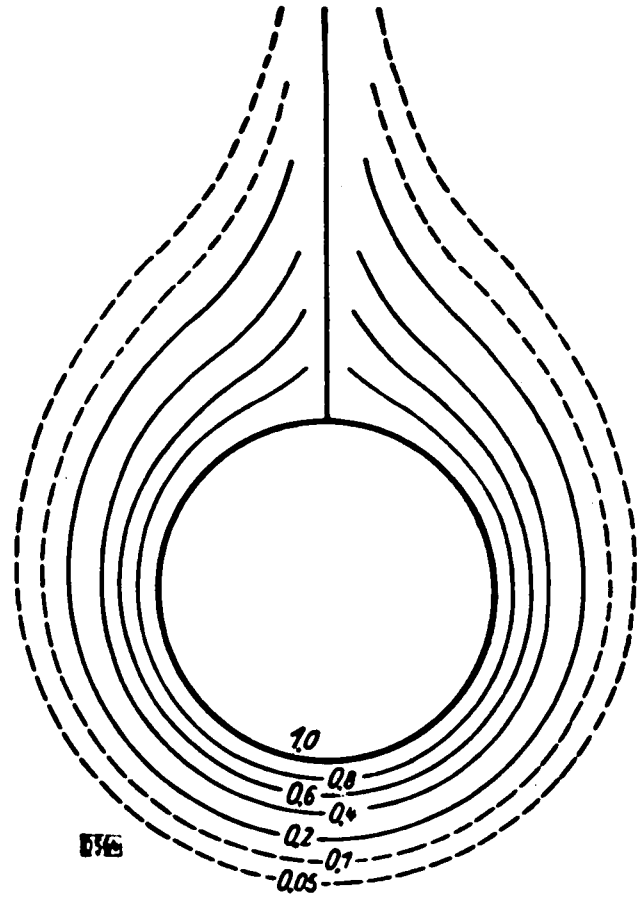

Figure 12. - Theoretical isotherms for horizontal cylinder. The numbers are values of θ/Θ. The scale is for Gr = 10^4, to be shortened as in figure 11 for other values of Gr.

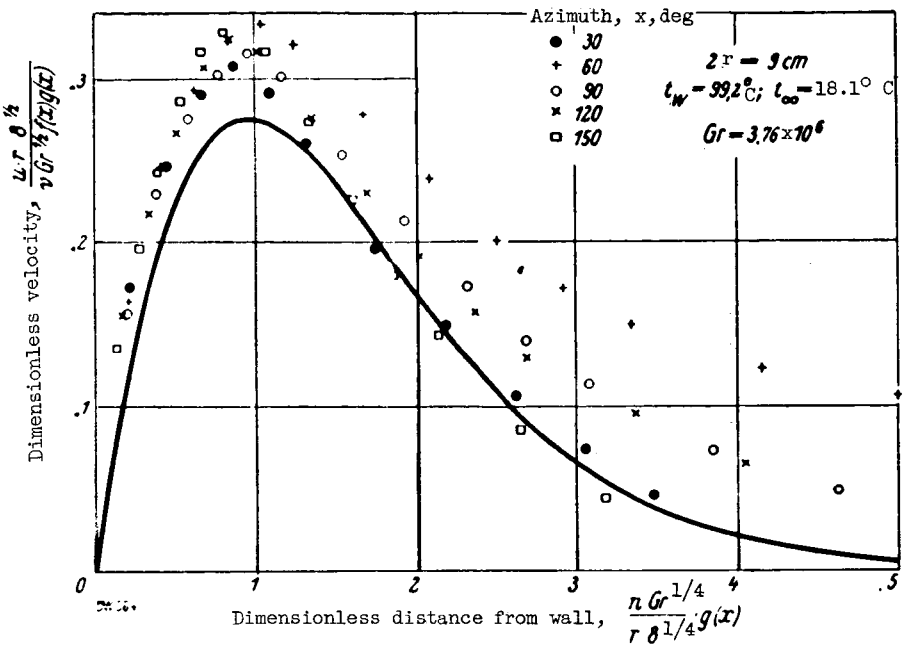

Figure 13. - Velocity profiles near cylinder referred to nondimensional coordinates. Continuous curve represents theoretical solution. Points according to measurements of Jodlbauer for 2r = 9 centimeters; t_w = 99.2° C; t_∞ = 18.1° C; Gr = 3.76x10^5.

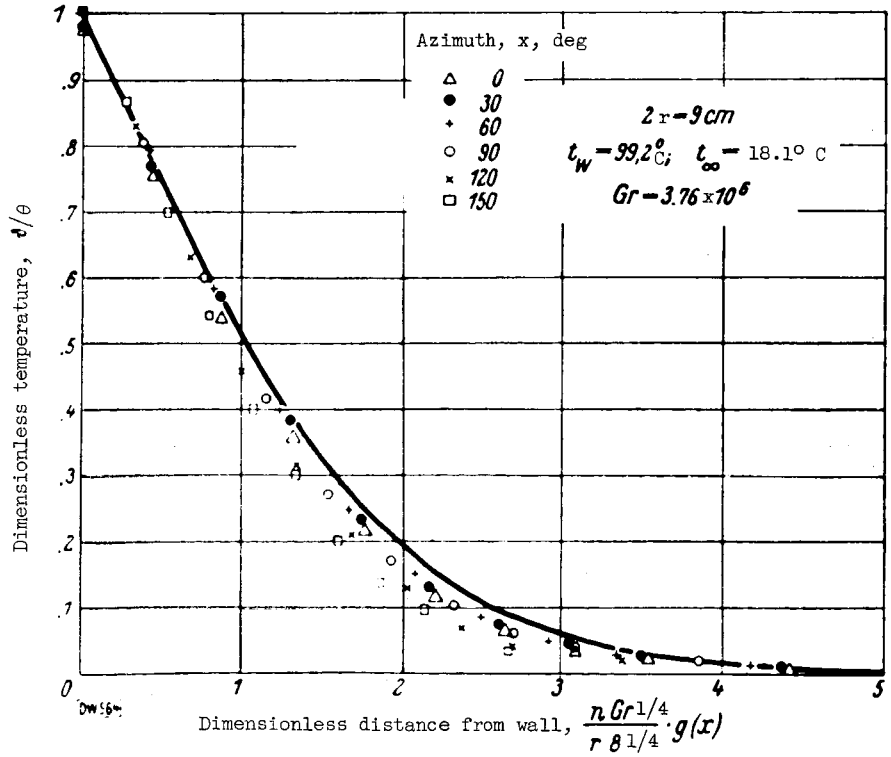

Figure 14. - Temperature profiles near cylinder referred to nondimensional coordinates. Continuous curve represents theoretical solution. Points according to measurements of Jodlbauer for 2r = 9 centimeters; t_w = 99.2° C; t_∞ = 18.1° C; Gr = 3.76x10^5.

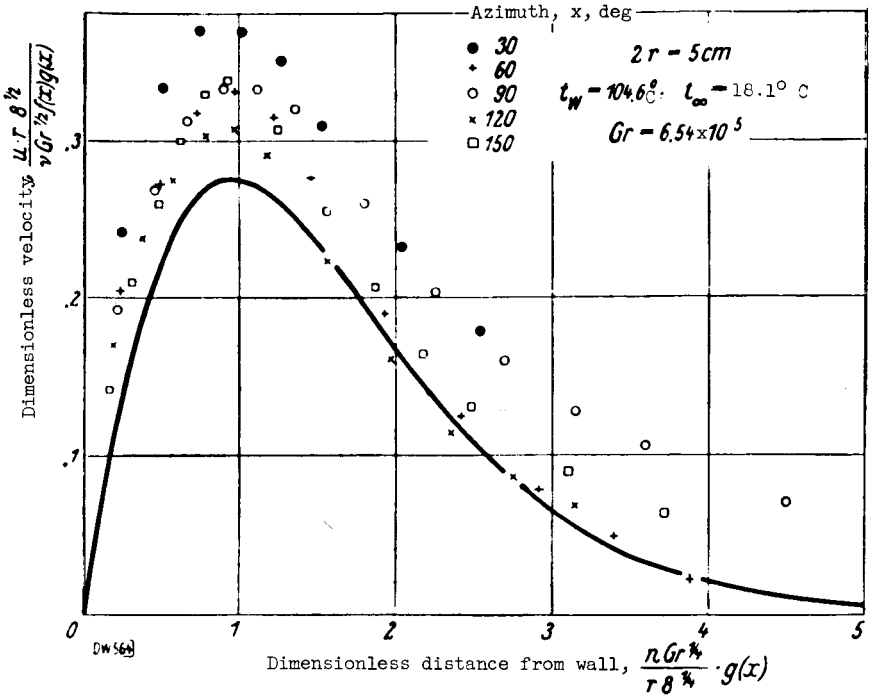

Figure 15. - Velocity profiles near cylinder. Continuous curve gives theoretical solution. Points according to measurements of Jodlbauer for 2r = 5 centimeters; t_w = 104.6° C; t_∞ = 18.1° C; Gr = 6.54x10^5.

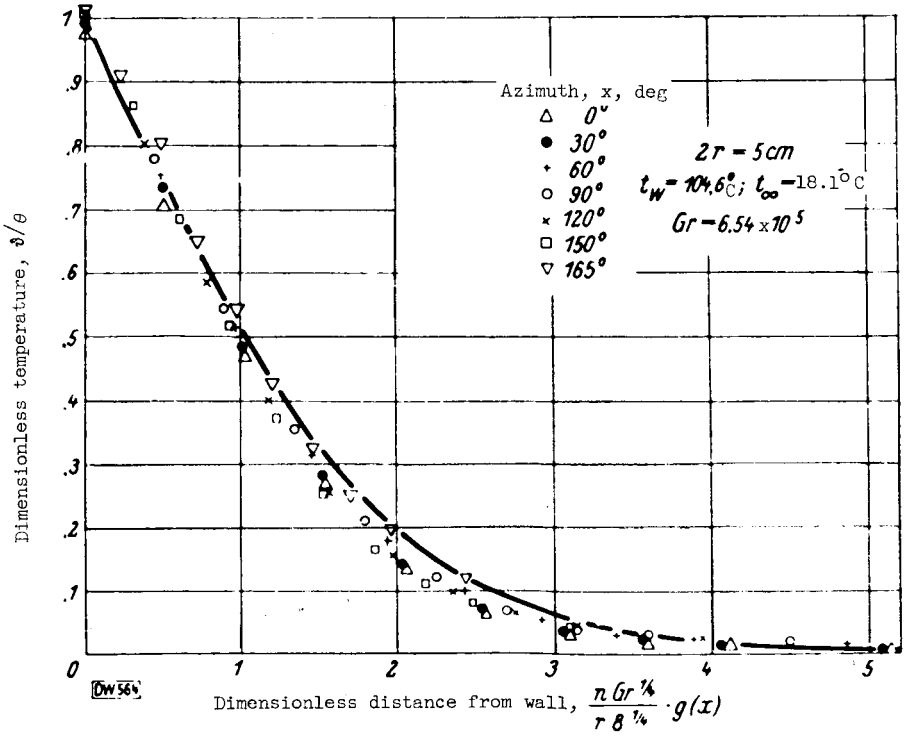

Figure 16. - Temperature profiles near cylinder. Continuous curve gives theoretical solution. Points according to measurements of Jodlbauer for 2r = 5 centimeters; t_w = 104.6° C; t_∞ = 18.1° C; Gr = 6.54x10^5.

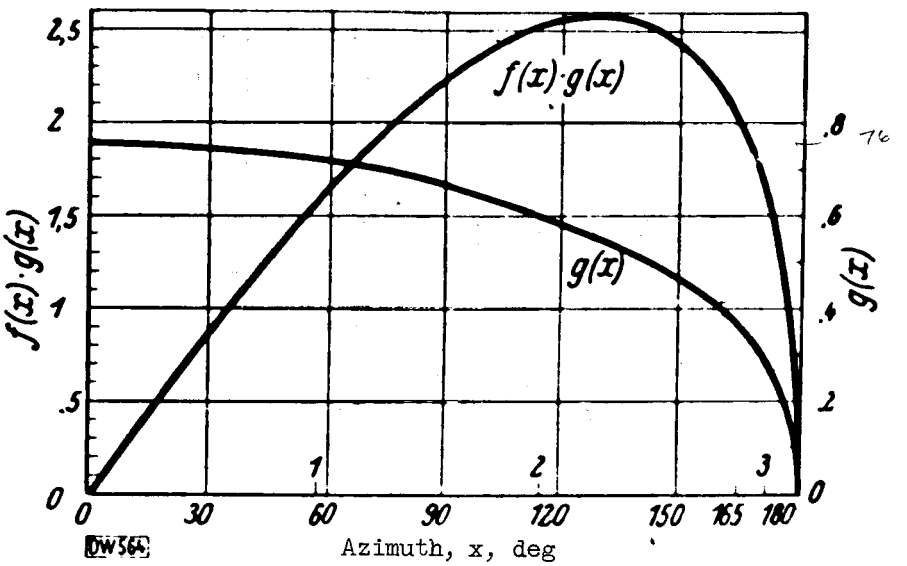

Figure 17. - Azimuth function g(x) giving variation of local heat-transfer coefficient or of a reciprocal distance from the wall which is characteristic for profile (for example, boundary-layer thickness) along cylinder perimeter.

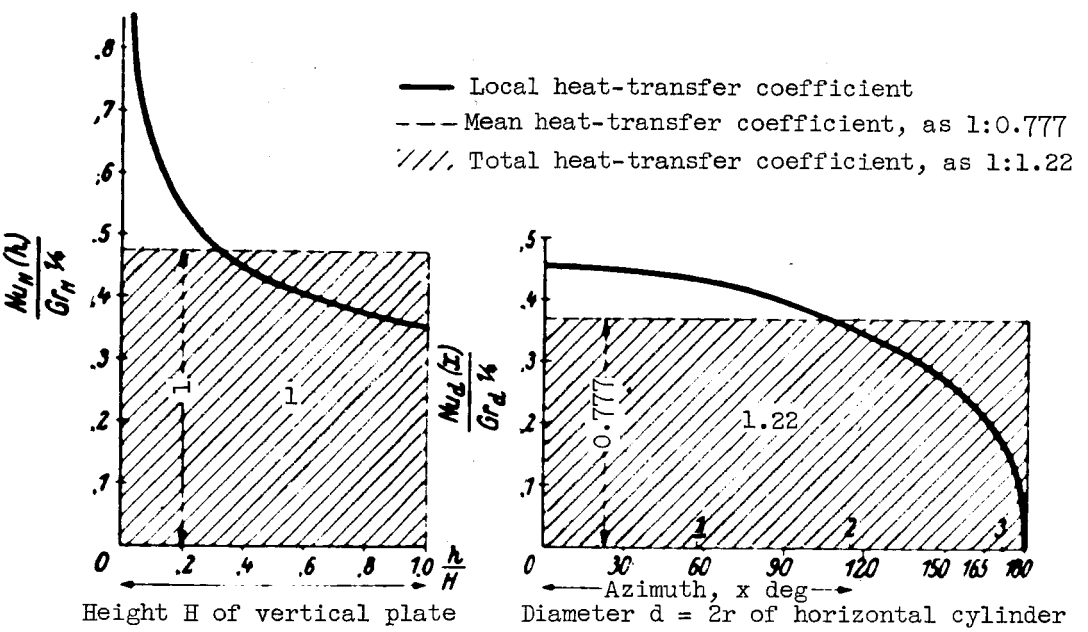

Figure 18. - Comparison of heat transfer for rectangular plate and horizontal cylinder. For H = d, under otherwise equal conditions, the two diagrams give dimensional heat-transfer coefficients α to scale.

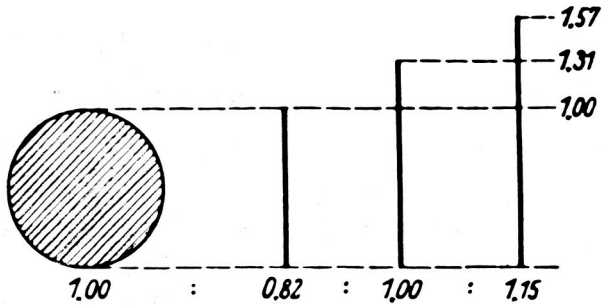

Figure 19. - Ratio of total heat transfer of horizontal cylinder and vertical plates (on both sides) of different heights under otherwise equal conditions. Ratio of boundary-layer Re at upper stagnation point of cylinder and upper edge of plate. Abscissa, heat transfer and Re; ordinate, plate height.

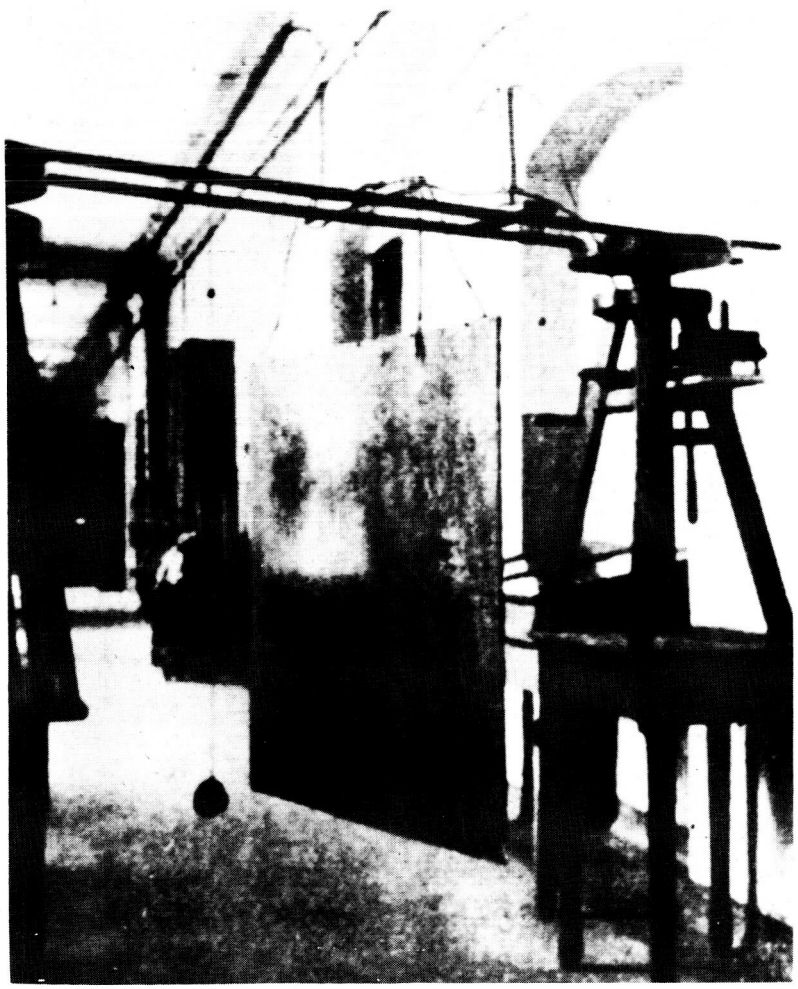

Figure 20. - Vertical plate 100x100x1 centimeters for determining occurrence of turbulence for free convection.

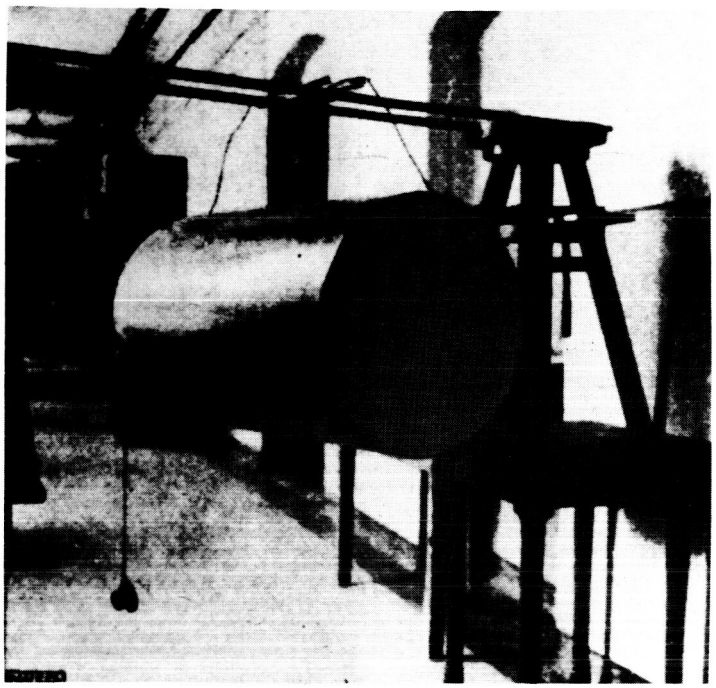

Figure 21. - Horizontal cylinder (58.5-cm diam., 100-cm length) for determining occurrence of turbulence for free convection.

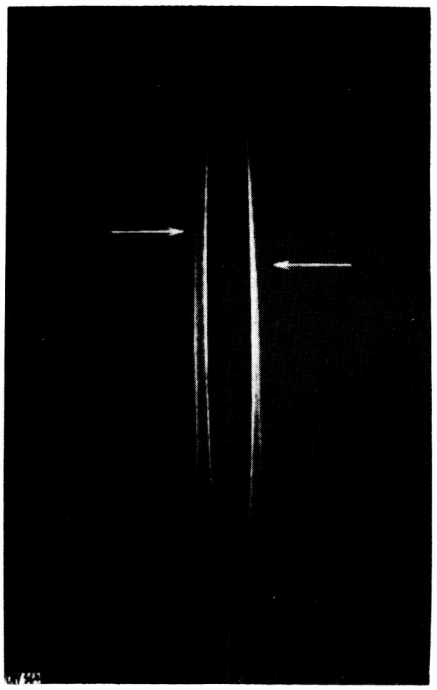

Figure 22. - Schlieren photograph of heat transfer at the vertical plate. Time photograph (25 sec) with lens and camera. Surface temperature, t_w = 100° C; t_∞ = 16.5° C; b = 748 millimeters; critical height (arrows), left 66.2 centimeters, right 60 centimeters; critical Grashof number, 13.1×10^8; critical boundary-layer Re, 323.

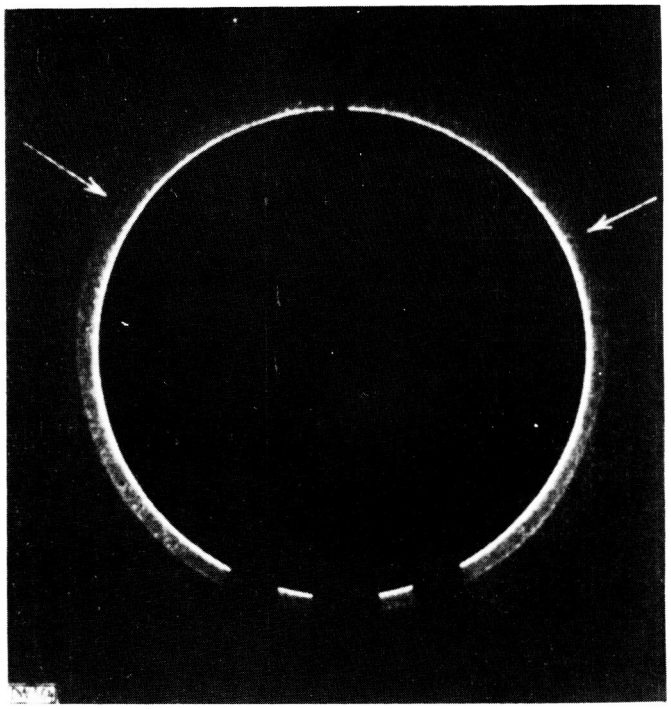

Figure 23. - Schlieren photograph of the heat transfer at the horizontal cylinder. Time photographs (20 sec) with lens and camera. t_w, 102° C; t_∞, 18° C; b, 752 millimeters; Gr of the cylinder, 10.2×10^8; critical azimuth (arrows) left 123.8°, right 115.0°; critical boundary-layer Re, 281.

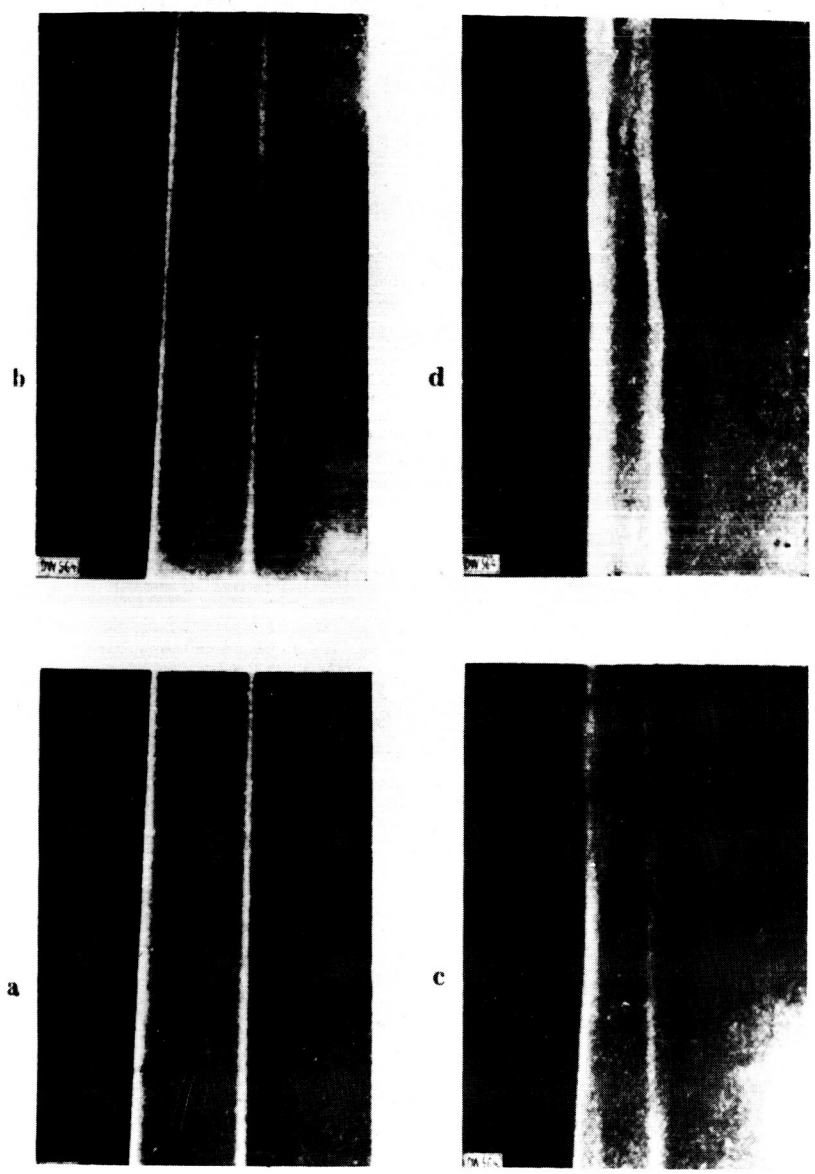

Figure 24. - Schlieren photographs of heat transfer at one side of vertical plate. Simultaneous instantaneous photographs (about 1/20 sec) with indirect illumination. t_w, 86° C; t_∞ 16.5° C; b = 748 millimeters. (a) laminar; upper part of (b), transition; (c) and (d), turbulent.

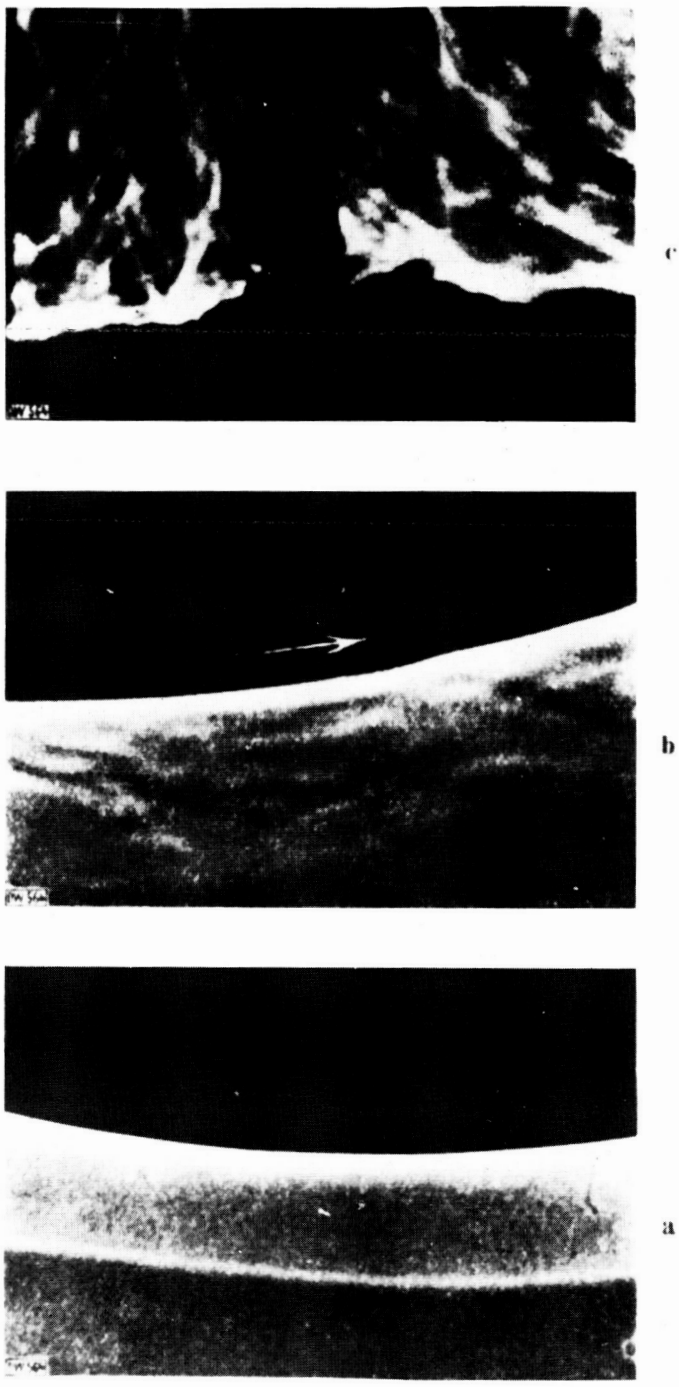

Figure 25. - Schlieren photographs of heat transfer at the horizontal cylinder. Simultaneous instantaneous photographs (1/20 sec) with indirect illumination. t_w = 102° C; t_∞ = 18° C; b = 752 millimeters; Gr, 10.2×10^8. (a) lower stagnation point, laminar; (b) azimuth of about 120°, turbulent; (c) upper stagnation point, upflow of warm air with current lead wires and so forth.

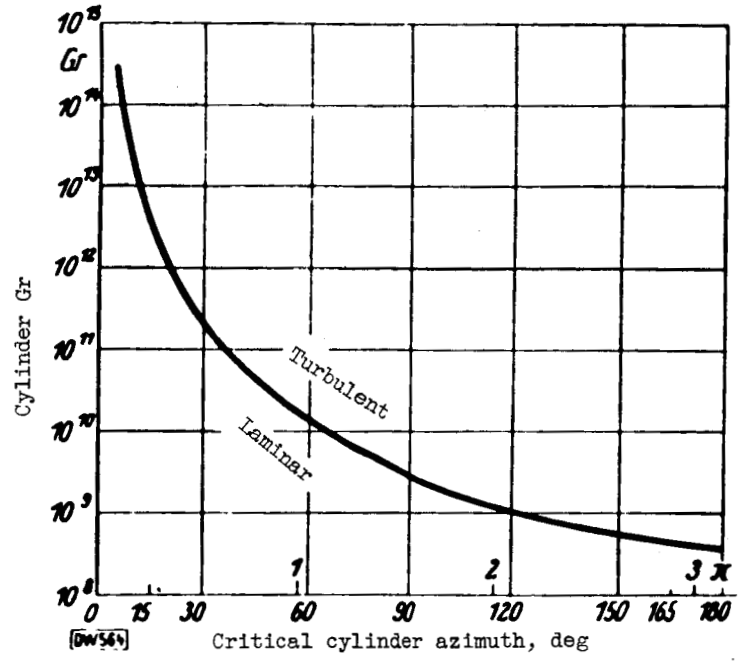

Figure 26. - Variation of position of start of turbulence with Gr number of cylinder. Computed for critical boundary-layer Re, 285.

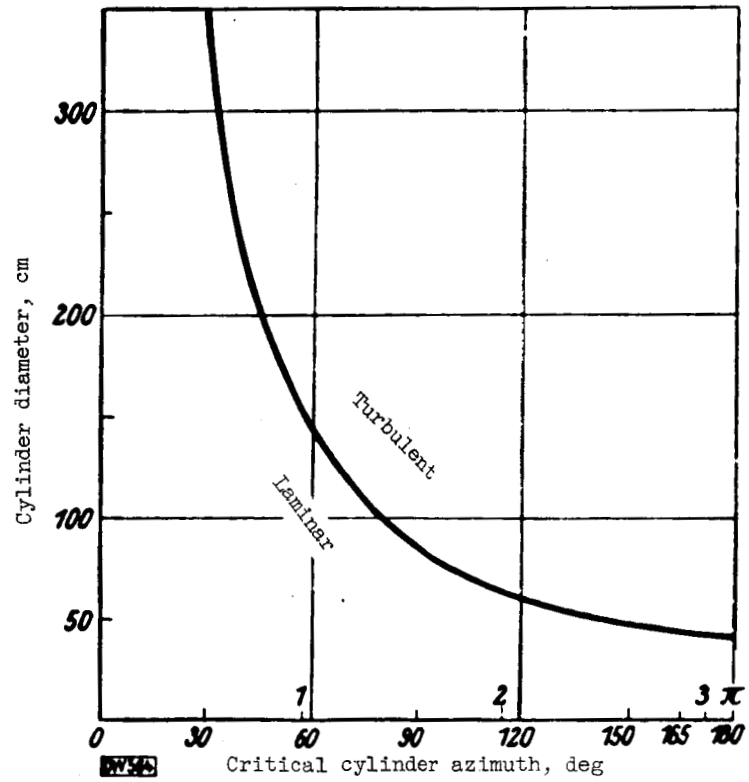

Figure 27. - Variation of position of start of turbulence with the cylinder diameter for surface temperature of 100° C in air at 20° C and 760 millimeters of mercury. Computed for critical boundary-layer Re, 285.

NACA-Langley - 11-3-54 - 1000